McNaughton, E., Eustace, A., King, S., Sessions, R., Kay, A., Farris, M., Kehoe, O., Kung, A., & Middleton, J. (2018). Novel anti-inflammatory peptides based on chemokine – glycosaminoglycan interactions reduce leukocyte migration and disease severity in a model of rheumatoid arthritis. *Journal of Immunology*, *200*(9), 3201-3217. https://doi.org/10.4049/jimmunol.1701187

Novel anti-inflammatory peptides based on chemokine – glycosaminoglycan interactions reduce leukocyte migration and disease severity in a model of rheumatoid arthritis

Emily F. McNaughton[*], Andrew D. Eustace[*], Sophie King[*], Richard B. Sessions[*], Alasdair Kay[§], Michele Farris[‡], Robert Broadbridge[‡], Oksana Kehoe[§], Andreas J. Kungl[†] & Jim Middleton[*]

[*] University of Bristol, UK

[§] University of Keele, UK

[‡] Peptide Protein Research Ltd, UK

[†] Karl-Franzens University, Austria

Corresponding author; email: jim.middleton@bristol.ac.uk

Author contributions: JM conceived and designed the study. EFM, ADE, SK, OK and AK performed experiments and analysed data. RBS assisted with peptide modelling and design. MF and RB provided peptide synthesis facilities and peptide chemistry consultation. AJK advised and contributed to IFT data. EFM and JM wrote the manuscript.

Funding was provided by the Biotechnology and Biological Sciences Research Council (BBSRC), Peptide Protein Research (PPR Ltd), Bristol Research into Alzheimer's and Care of the Elderly (BRACE) and British Microcirculation Society (BMS).

Abstract

Inflammation is characterised by the infiltration of leukocytes from the circulation and into the inflamed area. Leukocytes are guided throughout this process by chemokines. These are basic proteins which interact with leukocytes to initiate their activation and extravasation via chemokines receptors. This is enabled through chemokine immobilisation by glycosaminoglycans (GAGs) at the luminal endothelial surface of blood vessels. A specific stretch of basic amino acids on the chemokine, often at the C-terminus, interacts with the negatively charged GAGs which is considered an essential interaction for the chemokine function. Short chain peptides based on this GAG binding region of the chemokines CCL5, CXCL8 and CXCL12γ were synthesised using standard Fmoc chemistry. These peptides were found to bind to GAGs with high affinity which translated into a reduction of leukocyte migration across a cultured endothelial monolayer in response to chemokines. The leukocyte migration was inhibited upon removal of heparan sulphate (HS) from the endothelial surface and was found to reduce the ability of the chemokine and peptide to bind to endothelial cells in binding assays and to human rheumatoid arthritis (RA) tissue. Furthermore, control peptides lacking the basic amino acids showed reduced interaction with HS and no anti-chemotactic ability for leukocytes across an endothelial monolayer. The data suggest that the peptide competes with the wildtype (WT) chemokine for binding to GAGs such as HS and thereby reduces chemokine presentation and subsequent leukocyte migration. Furthermore, the lead peptide based on CXCL8 could reduce the disease severity and serum levels of the pro-inflammatory cytokine TNFα in a murine antigen induced arthritis model. Taken together, evidence is provided for interfering with the chemokine – GAG interaction as a relevant therapeutic approach. The use of site specific sequences of chemokines

to target GAGs and compete with WT chemokines is a novel and promising avenue for the field.

Introduction

Inflammation is a necessary process to prevent infection and the effects of injury on the body and its conclusion requires a controlled self-limiting process. When it becomes unresolved and chronic it becomes destructive leading to inflammatory disease. Leukocyte extravasation is a characteristic of inflammation and the recruitment of leukocytes from the circulation into the inflamed tissue is a multi-step process (1). Firstly, leukocytes are loosely tethered to the endothelium of blood vessel walls where they roll and interact with endothelial cell (EC) bound chemokines and adhesion molecules such as selectins. The interaction with chemokines activates leukocyte integrins enabling the leukocyte to mediate firm adhesion to the endothelium. Chemokines also stimulate leukocyte crawling on the endothelial surface and migration across the ECs, the basement membrane and into the extracellular matrix of the tissue (2). Once within the tissue, leukocytes normally perform various beneficial immune duties such as tissue repair and pathogen elimination. Due to the potentially destructive nature of leukocytes, tight regulation is required otherwise inflammatory disease can ensue. Chemokines play a role in the regulation of the inflammatory process by interactions with two binding molecules: G-protein coupled receptors (GPCRs) and GAGs.

Chemokines are small (8-10 kDa) chemoattractant cytokines involved in numerous physiological processes such as angiogenesis but mainly their role lies in the chemoattraction of migratory cells (3). Thus far, around 45 chemokines have been identified and are classified into four groups (C, CXC, CX3C and CC) based on the pattern of cysteine residues in the ligands (4). Despite the range and diversity of

chemokines with regards to their homeostatic or inflammatory function, they have a remarkably similar tertiary structure consisting of a conformationally disordered N-terminus, a long N-loop followed by a single turn 3_{10} helix, a three stranded antiparallel β-sheet and a C-terminal α-helix (5). The flexible N-terminal region is central to receptor activation since studies have shown that mutations or truncation of this region results in altered leukocyte activity (6, 7). *In vitro* studies have shown that more than one chemokine can bind to a given receptor and that several receptors are able to bind a given chemokine hinting that a large amount of redundancy takes place. However, *in vivo*, the interaction seems to be more specific, it has been suggested that chemokine "redundancy" is in fact more likely "finely tuned" (8). Different ligands can activate distinct signalling pathways following binding to the same receptor. For example, both CCL19 and CCL21 induce chemotaxis of CCR7 expressing cells, yet only CCL19 is able to induce receptor downregulation (9). As we learn more about chemokines, they may prove to be attractive therapeutic targets in the clinic.

The second and less well characterised interaction of chemokines is with carbohydrates, namely GAGs. GAGs are long, linear and heterogenous structures consisting of repeating disaccharide units which vary in the basic composition of the saccharide, the linkage to the core protein, acetylation and N- and O-sulphation (10). GAGs are ubiquitously expressed although different types (heparan-, dermatan-, chondroitin- and keratan- sulphate) may be found on cell surfaces within the glycocalyx and throughout the extracellular matrix of all mammalian tissues. GAGs can be surface bound or shed as soluble ectodomains (11); a process which dramatically changes their function (12). Their chain lengths can range from 1 to 25,000 disaccharide units thus together with structural variation in sulphation

patterns, this presents an immense level of diversity. This amount of diversity suggests an element of control and specificity when binding their biological ligands. GAGs are usually covalently attached to a protein core (with the exception of hyaluronic acid and heparin) to form a proteoglycan (PG). The most ubiquitous of these PGs are heparan sulphate proteoglycans (HSPGs) which are classified into 5 groups of core proteins which range in size from 32 to 500 kDa. The most abundant form are the syndecans that contain a transmembrane region anchoring them to the cell surface. In contrast, the glypicans are anchored to the cell surface via glycosyl-phosphatidylinositol groups and the other three (perlecan, agrin and collagen XVIII) do not have direct links to the cell membrane but remain closely associated with it (10). The composition and spacing of the GAG chains on the protein is dependent on the cell type and correlates with different physiological responses of the cell (13). The differential expression of PGs on particular cells allows them to dynamically function and adapt within the local microenvironment exhibiting an aspect of functional specificity.

GAG chains have been implicated in leukocyte transmigration and one GAG in particular is believed to have multiple roles in the extravasation process: heparan sulphate (HS) (14). HS is the most abundant endothelial GAG and composes 50-90% of total endothelial PGs (15). HS has been implicated in binding to a wide range of proteins some of which include cytokines, adhesion molecules, proteases and growth factors. Interaction of chemokines with HS can protect them from proteolysis (16) and induce them to oligomerise; high order oligomers are thought to be required for maximal chemokine activity (17). Furthermore, the interaction establishes chemokine gradients for migrating leukocytes by being bound and presented at the

endothelial luminal surface (18) and HS is involved in the transcytosis of chemokines across the EC layer to be displayed at the luminal surface (18). Leukocyte crawling also involves a chemokine – HS interaction and is critical for the leukocyte to find optimal sites to emigrate (2). One might consider the subendothelial basement membrane represents a formidable barrier to leukocyte extravasation, often being in the range of 20 nm -100 nm thick, yet it is also rich in extracellular HSPGs. This complex network of extracellular HSPGs such as perlecan, agrin and type XVIII collagen can serve to bind and sequester proteins that regulate leukocyte migration such as chemokines thereby contributing to leukocyte diapedesis (14). Hence chemokine interaction with HS is involved in several key stages of leukocyte extravasation.

The GAG binding motif on chemokines typically takes the form XBBXBX in CC chemokines (19) or XBBBXXBX in others where B represents a basic and X represents any non-basic amino acid (20). In general, these motifs are found in a separate location from the specific receptor binding domain, and often within the C-terminus. Although positively charged chemokines have a favourable charge interaction with negatively charged GAGs, several lines of evidence suggest that more than non-specific electrostatic forces drive this interaction. For example, acidic chemokines such as CCL3 and CCL4 also bind GAGs (21) and it is thought that specificity of the GAG-chemokine interaction is introduced by Van der Waals and hydrogen-bond forces (10). The GAG binding function of chemokines has been shown to be essential for optimal chemokine activity *in vivo* (19, 22-25). For example, when CXCL8 is truncated of its HS-binding C-terminal helix, it fails to bind heparin and has impaired leukocyte activation and receptor-binding properties (26).

The truncation also shows reduced transcytosis across endothelial cells and luminal surface presentation to blood leukocytes, resulting in reduced leukocyte transmigration (18, 27).

Chronic inflammation is also characterised by changes in GAG patterns (28). Changes in cell-surface and secreted GAGs in cancer has been shown to strongly influence the phenotype of the tumour, allowing them to control growth rates, invasiveness and metastatic potential (29). Moreover, a CXCL8 binding site on endothelial syndecan-3 is induced in the synovium of rheumatoid arthritis (RA) patients (30). Furthermore, in an animal model of RA, syndecan-3 functions in endothelial chemokine presentation and leukocyte recruitment suggesting a role for this HSPG in leukocyte trafficking into the inflamed tissue (31). Altered expression of endothelial GAGs has been observed in numerous other chronic inflammatory disorders including atherosclerosis (32) and inflammatory bowel disease (33). This could promote the binding and presentation of chemokines that are selective for the particular GAG sequences expressed therefore contributing to a site-specific localisation of chemokines (34). This suggests an element of control over the function of chemokines by HS.

Clearly the GAG binding capability of chemokines is of importance in the multitude of steps involved in leukocyte extravasation. The potentially specific and unique interactions that chemokines have with discrete GAG sequences are as yet largely unexplored. Due to the number of diseases in which chemokines have been implicated, blockade of chemokine function seems an attractive strategy. This study aims to obtain more insight into the GAG binding regions of particular chemokines

namely CCL5, CXCL8 and CXCL12γ and their functional roles. All of these chemokines are known to interact with HS and the HS binding domains are well established (20, 35, 36). These chemokines were chosen based on the cell types they interact with i.e. CCL5 is largely chemotactic for monocytes, CXCL8 for neutrophils and the relatively newly discovered CXCL12γ has a uniquely rich HS-binding C-terminus and appears to stimulate migration of lymphocytes. Using a novel approach, we chemically synthesised peptide chains based only on the GAG binding regions of each of these chemokines and tested their abilities to bind to HS and compete with chemokines in transendothelial migration assays. Sequences where the known HS binding residues including lysine and arginine were altered to non-charged residues such as glycine, serine and alanine were synthesised to act as controls. The lead peptide based on CXCL8 was assessed for binding to GAGs in EC lines and human RA synovium. It was then tested in a murine antigen induced arthritis (AIA) model. This strategy could improve future prospects for exploiting GAGs as therapeutic targets and other strategies for targeting chemokine-GAG interactions.

Materials and Methods

Peptide modelling

The crystal structures of each chemokine were taken from the Protein Data Bank (PDB): CXCL8 (PDB code: 3IL8), CCL5 (PDB code: P_1U4L) and CXCL12 (PDB code: 2NWG). Using the biopolymer module of molecular modelling program, Insight II (version 2005 by Accelrys), each of the chemokines was displayed and the peptides based on chemokines were structurally defined. The chemokines were rendered using a space-filling model (cpk representation) to represent the atoms present and are modelled as the biologically relevant dimers. Peptides based on chemokines were modelled to show the amino acid sequences of the peptide highlighted on the particular region of the chemokine where they are located. The structure of peptide (p)CXCL12-1 required the construction of C-terminal alpha helices found in the CXCL12γ isoform which were modelled onto residue 67 and extended to 98 residues. The design of pCXCL8-4 was based on the C-terminal alpha helices spliced together with a linker sequence GSGSG. The GNU image manipulation program (GIMP) version 2.8 was used to manipulate images and perform format conversion.

Peptide synthesis

All reagents and solvents for peptide synthesis were purchased commercially from Sigma-Aldrich, Gillingham, UK and peptides were synthesised at PPR Ltd, Bishops Waltham, UK. Solid phase peptide synthesis was carried out on an automated peptide synthesiser Symphony® employing standard Fmoc chemistry. Peptides were cleaved from the solid support and purified using reverse-phase HPLC. The crude peptide product was loaded onto a preparative C-18 Axia silica column typically running a

linear gradient of water and acetonitrile buffers, each containing 0.1% trifluoroacetic acid (TFA) at a gradient routinely run from 20% to 60% acetonitrile (depending on the peptide) for 1 hour at a flow rate of 20 ml/min whilst monitoring the eluent at 225 nm. The collected fractions were lyophilised before analytical techniques such as liquid chromatography – mass spectrometry (LCMS) were employed to give an overall purity read out. Peptides were > 90% pure. Peptide sequences can be seen in Table 1.

Some peptides were N-terminally modified by the addition of tags such as biotin and FITC (fluorescein isothiocyanate). These were coupled manually to the last amino acid of the N-terminus using an aminohexanoic acid (Ahx) linker overnight and the resulting peptide was cleaved from the resin as normal. The lead peptide pCXCL8-1 was capped at the C-terminus by using a resin functionalized with a modified Rink Amide linker and at the N-terminus with 50% acetic anhydride / pyridine in order to be used for intra-articular administration in vivo.

Isothermal fluorescent titration

The titration experiments were performed on a Fluoromax-4 Spectrofluorometer (Horiba, Kyoto, Japan) coupled to an external water bath to ensure constant temperature during the measurements. Protein fluorescence emission spectra were recorded over the range of 500 – 600 nm upon excitation at 495 nm. The slit widths were set at 3 nm for excitation and emission, scan speed at 500 nm/min and the temperature was set to 20°C. The use of concentrated GAG oligosaccharide stock solutions ensured a dilution of the protein sample less than 5%. Prior to collection of the initial (=unliganded) protein emission spectra, 100 nM protein solutions were

prepared from stock solutions and were equilibrated for 30 mins. Following equilibration, respective GAG ligands (HS [catalogue number: GAG-HS01], DS [catalogue number: GAG-DS01]; Iduron Manchester, UK) were added in concentrations ranging from 5 nM to 50 nM. The protein / GAG solutions were then equilibrated for 1 min and fluorescence emission spectra were collected. For background correction the emission spectra of the respective GAG concentrations were collected in PBS buffer only. They were subsequently subtracted from protein emission spectra and the resulting curves were then integrated. The mean values resulting from 3 independent measurements were plotted against the concentration of the added ligand. The resulting binding isotherms were analysed by non-linear regression using the program Origin (Microcal Inc., Northampton, MA, USA) to the following equation describing a bimolecular association reaction, where Fi is the initial and Fmax is the maximum fluorescence value. K_d is the dissociation constant, and [protein] and [ligand] are the total concentrations of the chemokine/peptide and the GAG ligand:

$$F = F_i + F_{max}\left[\frac{K_d + [protein] + [ligand] - \sqrt{(K_d + [protein] + [ligand])^2 - 4[protein][ligand]}}{2[protein]}\right]$$

Cell culture

Immortalised human bone marrow ECs (HBMECs), and human cerebral microvascular ECs (HCMEC/D3s) were both donated by Prof B. B Weksler, Cornell University, New York and support leukocyte transendothelial migration studies (37-39). HBMECs were maintained in DMEM-F12 (Lonza, Wokingham, UK) supplemented with 10% FBS (Invitrogen, Paisley, UK) and HCMEC/D3s in rat tail collagen type 1 (R&D Systems, Abingdon, UK) coated flasks (150 mg/ml in dH_2O) using EBM-2 (Lonza) containing 1% penicillin-streptomycin (Invitrogen), 1% chemically defined lipid concentrate (Invitrogen), 1 ng/ml basic fibroblast growth

factor (bFGF; Sigma-Aldrich), 1.4 μM hydrocortisone (Sigma-Aldrich), 5 μg/ml ascorbic acid (Sigma-Aldrich), 10 mM HEPES (PAA Laboratories, Yeovil, UK), 5% FBS and 10 mM lithium chloride (Merck, Feltham, UK). All ECs were incubated at 37°C in a humidified incubator containing 5% CO_2. Cells were grown to 70% confluence before being used in the following experiments.

HS Immunofluorescence

ECs were seeded at a density of $2.5x10^5$ in Nunc® Lab-Tek® 8-well chamber slides (Sigma-Aldrich) using 500 μl serum free medium and left to reach confluence for 24 hours. Some cells were treated with heparanase I (10 U/ml) and heparanase III (2 U/ml; both from Sigma-Aldrich) as described by Whittall et al, (2013) for 1.5 hours at 37°C to remove the HS. Following the heparanase treatment cells were fixed with 4% PFA for 10 mins before being incubated with 2 μg/ml mouse anti-human HS antibody (10e4; AMSBio, Abingdon, UK) for 1 hour in 2% BSA/PBS at room temperature (RT). The cells were washed 3 times in PBS. The primary antibody was detected by Alexa Fluor 488 goat anti-mouse IgM (1:200 in 2% BSA/PBS) and the cells washed before being counterstained in DAPI (2 μg/ml; 4',6-diamidino-2-phenylindole) for 3 mins. For a control, mouse IgM was used at an equivalent concentration in place of the primary antibody. Slides were mounted using Hydromount (Fisher Scientific, Loughborough, UK) and visualised with a light fluorescence microscope (Leica DM LB) and analysed with Cell^D software.

Transendothelial migration

Leukocyte isolation

For all leukocyte collection, a total of 20 ml blood was collected from healthy volunteers, after informed consent, into lithium heparin treated vacutainers. To isolate polymorphonuclear (PMNs) cells the blood was centrifuged at 500 x g for 30 mins with polymorphprep (Axis-Shield, Oslo, Norway) followed by the removal of mononuclear (MNs) cells and erythrocytes. The remaining PMNs were washed with an equal volume of HBSS and dH_2O for 10 mins at 400 x g followed by erythrocyte lysis using ammonium chloride solution (Stemcell Technologies, Cambridge, UK) for 7 mins at 37˚C. The PMNs were then harvested by centrifugation at 300 x g for 5 mins, resuspended in 0.1% BSA in RPMI-1640 (Lonza) and held at 4˚C until required. For mononuclear cell isolation, the same process applied except the MNs were harvested after initial centrifugation and the PMNs and erythrocytes were discarded.

Neutrophil migration through an endothelial layer

A total of 2.5 x 10^5 ECs in 500 µl cell growth medium were cultured on 3 µm pore transwell filters (Fisher Scientific) in a 24-well flat-bottomed microplate (Corning® Costar®, Sigma-Aldrich) with 800 µl of cell growth medium in the basal chambers until confluence was reached (24 hours at 37°C). The solution in the apical chamber was replaced with 500 µl fresh serum-free medium and the solution in the basal chamber was replaced with a solution of serum-free medium containing 100 ng/ml CXCL8 or CXCL12γ; for controls, serum-free medium containing no CXCL8 or CXCL12γ was used. The samples were incubated at 37°C for 30 mins for endothelial activation to occur as described by Whittall et al. 2013. ECs were activated by incubating monolayers with the following chemokines: recombinant human CXCL8, CCL5 (both from Peprotech) and CXCL12γ (R&D Systems) at concentrations of 100

ng/ml in serum free medium for 30 mins at 37°C (39). The negative controls contained no chemokines. Monolayers were established by optimising seeding density of ECs and allowing to reach confluence over 24 hours. At this time point the trans endothelial electrical resistance (TEER) value was maximum (using an EVOM2 voltmeter) and experiments were carried out identically thereafter. A total of 5×10^5 PMNs were then added to the apical chambers, followed by incubation at 37°C for a further 30 mins in continued presence of CXCL8 or CXCL12γ. PMN migration was quantified by determining the number of neutrophils that had migrated through to the basal chamber in 30 mins by manual counting using a disposable haemocytometer (Immune Systems, Torquay, UK) and displayed as a percentage of transendothelial migration when compared to chemokine alone.

Mononuclear cell migration through an endothelial layer

MN cell migration was carried out in an identical manner to PMN cell migration with three notable differences. The chemokine was human recombinant CCL5 (100 ng/ml), the ECs were cultured on 5 μm pore transwell filters (Fisher Scientific) and a total of 4×10^5 MNs were added to the apical chamber, followed by incubation at 37°C for 3 hours following addition of MNs in continued presence of CCL5.

Inhibiting leukocyte migration using peptides

To assess the ability of peptides based on CXCL8, CXCL12γ and CCL5 to inhibit leukocyte migration, a range of concentrations (0.5, 5, 50, 500 and 5000 nM) were added to the basal chamber of the transwell system at the same time as the corresponding chemokine. Serum-free medium containing chemokine alone was used as the positive control and containing no chemokine as the negative control. The

ability of the test peptide at inhibiting leukocyte migration was also compared with a peptide control (Table 1; a sequence containing charged HS binding sites i.e. Lys and Arg to non-charged amino acids i.e. Ala, Gly or Ser) using the HCMEC/D3 cell line.

Inhibiting leukocyte migration using heparanases

To assess the role of HS in leukocyte migration, ECs in the transwell chambers were treated with heparanase I and III as described above and by (39). Following incubation with heparanases, relevant chemokines were added and leukocyte transendothelial migration was carried out as before.

ELISA-like competition assay

GAG binding plates (Iduron) were coated with 25 µg/ml of HS (Sigma: catalogue number H7640-10MG) in standard assay buffer (100 mM NaCl, 50 mM sodium acetate, 0.2% v/v Tween 20, pH 7.2) overnight at RT. After washing the plate three times with standard assay buffer, the wells were blocked with blocking solution (1% w/v BSA in PBS) for 1 hour at 37°C and the wash step repeated. CXCL8 (Peprotech, London, UK) was titrated for detection and used thereafter at 0.75 µg/ml in blocking solution. CXCL8 was incubated with different competitor concentrations of peptide (pCXCL8-1: 0.5, 5, 50, 500, 5000 nM) for 2 hours at 37°C in triplicate. Unbound chemokine and peptide was removed by three wash steps followed by addition of a 220 ng/ml solution of biotinylated anti-human CXCL8 (Peprotech) in blocking solution for one hour at 37°C. Following three more washes, 220 ng/ml ExtrAvidin-alkaline phosphatase (Sigma) in blocking solution was added to the wells for 30 mins at 37°C. The plate was washed three times then 200µl of a development reagent, SigmaFAST p-Nitrophenyl phosphate (Sigma) was added and left to develop for 40

mins at RT. The optical density (OD) was then read at 405 nm using a spectrophotometer. Percentage inhibition of chemokine binding to HS was calculated as follows, with the control being standard assay buffer only:

$$\text{Percentage inhibition} = \frac{\text{OD (x nM chemokine + y nM peptide)} - \text{OD (control sample)}}{\text{OD (x nM chemokine)} - \text{OD (control sample)}} \times 100$$

Cellular binding assays by flow cytometry

ECs were detached from T75 flasks and incubated with labelled chemokine or peptide in FACs buffer (1% BSA/PBS) for 1 hour on ice. The peptide was titrated and used at 5 µg/ml of FITC labelled pCXCL8-1 (*f*pCXCL8-1) or control pCXCL8-1c (*f*pCXCL8-1c).

To assess CXCL8 binding to ECs, CXCL8 was labelled with Atto 425 (Bio-Techne, Abingdon, UK) according to the manufacturers instructions. The fluorescently labelled CXCL8 was titrated and subsequently used at 50 µg/ml (5.3 nM) in FACs buffer. For a control cells were incubated with FACs buffer only. Binding to ECs was carried out as before, for 1 hour on ice. In order to assess whether pCXCL8-1 could compete with CXCL8 for binding sites, 0.5 nM, 5 nM and 50 nM of unlabelled peptide was added at the same time as fluorescent CXCL8.

To confirm whether CXCL8 and the peptide pCXCL8-1 was binding to HS, cells were pre-treated with heparanase I and III as described previously (39) before the addition of fluorescently labelled CXCL8 or peptide.

Following the incubations cells were washed by spinning down with FACs buffer twice at 500 x g for 5 mins. Cells were then analysed for binding using a NovoCyte® flow cytometer and analysed using NovoExpress® software. Cells were gated on forward scatter side scatter on all viable cells and then a second gate was placed on singlets. To assess binding, forward scatter-area and FITC-area were used to gate on positive and negative cells of peptide binding and BV510-area was used to detect Atto425 emission of CXCL8 binding.

Tissue binding assays *in situ*

Synovial tissue was obtained from Keele University with full ethical approval from the Birmingham, East, North and Solihull Research Ethics Committee (study ID: 11/WM/0035). Sections were cut at 10 µm using a cryostat and mounted onto polylysine slides (Thermo Fisher) and stored at -20°C until use.

Sections were equilibrated at RT for 30 mins prior to use and then with ice cold binding buffer (0.1% BSA in HBSS containing 10 mM HEPES) for 5 mins. Labelled peptide and chemokine were added for one hour in binding buffer and these were biotinylated pCXCL8-1 (*b*pCXCL8-1; 5 µg/ml) which was detected with streptavidin Alexa Fluor 488 (1:200; BioLegend, London, UK) and Atto 425 (Bio-Techne) labelled CXCL8 (5 µg/ml/0.53 nM); Peprotech). In each case a double stain was performed with Von Willebrand factor antibody (15.5 µg/ml; DAKO, Cambridge, UK) followed by a goat anti-rabbit Alexa Fluor 594 (1:400; Thermo Fisher). For controls, binding buffer in the absence of *b*pCXCL8-1 and Atto 425 labelled CXCL8 were used and rabbit IgG (15.5 µg/ml; DAKO) in the place of anti-Von Willebrand factor.

In order to assess whether pCXCL8-1 could compete with CXCL8 for binding sites, an equimolar amount of unlabelled pCXCL8-1 (0.5nM) was added at the same time as Atto 425 labelled CXCL8. To confirm whether CXCL8 was binding to HS, tissue was pre-treated with heparanase I and III, as described previously (40), before the addition of labelled CXCL8. For a control, tissue was treated with binding buffer only.

Finally, sections were washed in binding buffer and then counterstained with DAPI (2µg/ml in dH_2O) for 5 mins. Sections were rinsed, mounted in Hydromount (Thermo Fisher) and visualised with a fluorescence light microscope (Leica DM LB) and analysed with Cell^D software.

Murine antigen induced arthritis (AIA)

Animals

Experiments were conducted in 7 to 10 - week-old inbred male C57Bl/6 WT mice. Animals were housed and maintained under conventional management at animal facilities at Liverpool John Moores University, UK. Procedures were performed with ethical approval from the Home Office, UK, and were carried out under the project licence PPL 40/3047.

Induction of murine AIA

Murine AIA was induced as described previously (31, 41). All reagents used for AIA induction were from Sigma-Aldrich. In short, mice were immunised subcutaneously with 1 mg/ml of methylated BSA (mBSA) emulsified with an equal volume of

Freund's complete adjuvant and injected intraperitonealy with 100 µl heat-inactivated Bordetella pertussis toxin, the subsequent immune response was boosted one week later. Three weeks after the initial immunisation, AIA was induced by intra-articular injection of 10 mg/ml mBSA into the right knee joint and PBS into the left knee joint to serve as a control.

Intra-articular injection of pCXCL8-1$_{aa}$

6 hours post arthritis induction, 10 µl of peptide (pCXCL8-1aa) (5 µg) and control peptide (pCXCL8-1c$_{aa}$) were injected intra-articularly (0.5 ml monoject (29G) insulin syringe, BD Micro-Fine, Franklyn Lakes, USA) into the right knee of 10 animals respectively. At the end of experiments (day 3 and day 7 post induction of AIA, n=5) animals were sacrificed and joints were collected for histology.

Histological assessment

Joints were fixed in neutral buffered formal saline and decalcified with 10% formic acid for 72 hours before embedding in paraffin. Mid-sagittal sections (2µm thickness) were cut and stained with haematoxylin and eosin (H&E) for scoring of degree of infiltration (normal = 0 – severe = 5), synovial hyperplasia in the lining layer (0-3) and cellular exudate in the joint space (0-3) as described previously (31, 41). Sections were stained with toluidine blue for scoring of degree of cartilage depletion (0-3) based on PG loss. Blind scoring was undertaken and all parameters were pooled to give an arthritic index (mean ± SEM).

Neutrophil infiltration was quantitated by counting the number of neutrophils in the synovium in H&E sections in 5 random fields of view at x1000 magnification as described previously (31). Means and standard errors were then calculated.

TNFα assay

Using a mouse TNFα ELISA Ready-SET-Go! Kit (eBioscience, Altrincham, UK) the serum concentration of TNFα was measured according to the manufacturer's instructions.

Statistical analysis

Statistical analysis was carried out on GraphPad Prism 5.0. A one-way ANOVA followed by Dunnett's post hoc test was used for multiple comparisons and a two-tailed Student's t-test for comparisons of two variables. p-values less than 0.05 were deemed as significant.

Results

Modelling and synthesising peptides based on the HS-rich binding domain of chemokines

Chemokines were chosen based on the cells they interact with and their roles in acute or chronic phases of inflammatory diseases. CXCL8 (Figure 1A) is a potent chemoattractant of neutrophils, CCL5 (Figure 1E) is largely associated with the chemotaxis of monocytes and T cells, and CXCL12γ (Figure 1G) for lymphocytes, the dysregulation of each resulting in upregulated leukocyte migration. The residues of the chemokines implicated in GAG binding have been shown to be contained within the C-terminal alpha helix of CXCL8 (35) and CXCL12γ (36) and within the 40s loop of CCL5 (20). Therefore, our peptides were modelled on these particular regions without the inclusion of the tertiary chemokine structure. In addition, control peptides were synthesised whereby the positively charged amino acids such as lysine and arginine were substituted with non-charged amino acids such as alanine, glycine and / or serine. The sequences can be seen in Table 1.

A number of CXCL8 peptides were modelled to include varying amounts of HS binding domains. A 10 amino acid peptide (pCXCL8-1) and a 15 amino acid peptide (pCXCL8-2) were synthesised based on the C-terminal alpha helix and included Lys^{64}, Lys^{67} and Arg^{68} (pCXCL8-1) plus the addition of Arg^{60} in pCXCL8-2 as seen in Figure 1B. CXCL8 also has another HS binding domain located within the proximal loop: Lys^{20}. Therefore, a longer 54 amino acid peptide was synthesised to include all of these HS binding sites (pCXCL8-3; Figure 1C). As CXCL8 exists in both monomeric and dimeric form, a further dimeric peptide was modelled to include

both alpha helices held in place with a linker molecule as seen in Figure 1D, comprising 41 amino acids in total (pCXCL8-4). Hence, this peptide therefore had a total of 8 HS binding sites. The lead peptide pCXCL8-1 was modified for *in vivo* work (pCXCL8-1_{aa}) in order to protect it from proteolytic degradation and reduced half-life. Due to the direct intra-articular administration of the peptide it was decided that the peptide would not need increased plasma half-life so instead it was opted to protect the peptide at the terminal regions. In order to do this, the peptide was amidated and acetylated thereby altering the peptide ends into an uncharged state (Table 1). This more closely mimics the native protein and these modifications would increase the metabolic stability of the peptide as well as its ability to resist enzymatic degradation.

Peptides based on CCL5 were chosen to include varying amounts of the 40s loop. Three peptides in total were designed. pCCL5-1 comprised four amino acids ^{44}RKNR^{47} and this was extended in the N-terminal direction to include Thr^{43} (pCCL5-2; five amino acids) and Val^{42} (pCCL5-3; six residues) as seen in Figure 1F and Table 1.

The peptide based on CXCL12γ (pCXCL12-1) takes advantage of its enriched C-terminal alpha helix. The 30 amino acid helix contains 18 basic residues, 9 of which are clustered into 4 acknowledged HS-binding domains and therefore the design for the peptide was simply to incorporate the 30 amino acids of this unique C-terminus (Figure 1H and Table 1).

Peptides based on chemokines bind to HS with high affinity

The affinity of the peptide interaction with HS and DS was determined by isothermal fluorescent titration. Peptides or intact chemokine were labelled on the N-terminus with FITC (*f*) and fluorescence quenching was measured upon interaction with HS or DS. This was repeated for control peptides where the putative HS binding sites had been altered to non-charged amino acids such as glycine, serine and alanine (Table 1). The resulting binding isotherms (Figure 2) were analysed by non-linear regression giving the K_d values shown in Table 2.

All measured *f*CXCL8 peptides gave a higher affinity (lower K_d) than WT *f*CXCL8. WT *f*CXCL8 bound to HS with a K_d of 128 nM whereas *f*pCXCL8-1 and -2 gave values of 15 nM and 61 nM respectively. The modified version of *f*pCXCL8-1 (*f*pCXCL8-1_{aa}) bound tighter than WT *f*CXCL8 although weaker than *f*pCXCL8-1 (by approximately 4 fold), which is attributed to the modifications at the N- and C-termini. Interestingly *f*pCXCL8-1, with 3 HS binding domains, had a 4 fold higher affinity for HS than *f*pCXCL8-2, with 4 HS binding domains. *f*pCXCL8-1 also exhibited some selectivity for HS over DS (15 nM compared with 44 nM) similar behaviour to WT *f*CXCL8, whereas *f*pCXCL8-2 binds with similar affinity to both (61 nM compared to 52 nM). Control peptides for *f*pCXCL8-1, *f*pCXCL8-1_{aa} and *f*pCXCL8-2 showed no significant interaction with HS (Figure 2B-D) and therefore no K_d values could be calculated. Quenching around 10% and late saturation of FITC fluorescence is indicative of a very weak and / or a non-specific interaction, thus highlighting the importance of the positively charged amino acids for GAG interaction.

The peptide based on CCL5, pCCL5-3, exhibited a strong affinity for HS with a K_d value of 8 nM. This peptide showed selectivity for HS over DS (8 nM compared to 148 nM). As can be seen in Figure 2E, the control peptide showed <10% FITC quenching, again highlighting the importance of the positively charged amino acids associated with GAG binding.

Due to the unique C-terminus of CXCL12γ, one would assume strong affinity for GAGs as confirmed by IFT measurements. pCXCL12-1 gave a K_d values of 2 nM and 3 nM to HS and DS respectively (Figure 2F). Interestingly, the control peptide for pCXCL12-1 showed some interaction with HS as indicated by the initial increase of the curve. However, this interaction appeared to be non-specific due to the lack of saturation of FITC fluorescence. The control peptide did contain positively charged amino acids that are reported to be uninvolved with GAG binding however these could be giving rise to some interaction with HS seen here.

HS is a key player in leukocyte migration and for chemokine binding

Before assessing the ability of peptides to bind to cellular HS and prevent leukocyte migration, it was necessary to determine the distribution of HS on ECs and elucidate the importance of this GAG during leukocyte transendothelial migration. The distribution of HS was examined by immunofluorescence as seen in Figure 3A and B which shows a mesh-work like pattern of HS on the cellular surface. When the cells were pre-treated with the enzymes heparanase I & III to degrade HS, the mesh-work like pattern was lost indicating a loss of HS on the cell surface (Figure 3C and D). As a control, cells were stained with an IgM isotype control.

To examine the function of HS in leukocyte transendothelial migration, ECs were pre-treated as before with HS degrading enzymes and leukocytes were then assessed for chemotaxis in response to chemokine in the basal chamber. Chemokine concentrations were titrated (0-500 ng/ml) and used at 100 ng/ml. As can be seen in Figure 3E, neutrophil migration was significantly reduced when treated with heparanase I & III compared to CXCL8 alone ($p < 0.0001$). The amount of neutrophil migration was equivalent to baseline in the absence of CXCL8 (data not shown). However, when assessing the effect of heparanase treatment on the migration of monocytes to CCL5 (100 ng/ml), a lesser role for HS was observed although still significant ($p = 0.0017$). From Figure 3F it can be seen that monocyte migration was reduced when HS was removed, however this reduction was ~40% compared to the 80% for neutrophils.

It is well established that GAGs are important in the binding and presentation of chemokines on the luminal surface of ECs (18, 27). To assess whether this is the case for our EC transwell system we pre-treated ECs with heparanases and then tested the binding of fluorescently labelled CXCL8 or pCXCL8-1 by flow cytometry. As can be seen in Figure 3G, CXCL8 bound to HCMEC/D3 cells significantly more than the control (FACs buffer only), exhibiting a total value of ~40% positive cells. When the HCMEC/D3s were pre-treated with heparanase I&III, the number of CXCL8 positive cells was significantly reduced ($p < 0.001$). These data agree with findings in Figure 3E; that HS is crucial for the binding and presentation of CXCL8. After confirming this was the case, we then wanted to see if the same was true for the peptide pCXCL8-1. This peptide exhibited almost 100% binding to HCMEC/D3 cells whereas the control pCXCL8-1c showed no binding (Figure 3H), this again highlights

the importance of the positively charged HS binding domains in the peptide for EC interaction. This also agrees with IFT data that pCXCL8-1 has a higher affinity for HS than CXCL8 by the fact that pCXCL8-1 binds with a 2.5 fold increase in the percent of EC binding compared to CXCL8 (Figure 3G and H). When the cells were treated with heparanases, the percentage positivity of pCXCL8-1 binding was significantly reduced ($p<0.001$) (Figure 3H).

Peptides reduce leukocyte migration through an EC layer

To characterise the anti-chemotactic ability of peptides based on chemokines, they were tested in an *in vitro* model of inflammation. Using a transendothelial cell assay in two cell lines, the ability of the peptide to prevent leukocyte migration towards a chemokine stimulus was measured (Figure 4). pCXCL8-1 significantly reduced neutrophil migration in the HCMEC/D3 cell line compared to the corresponding control peptide (Table 1) at all concentrations of peptide apart from 5000nM. The optimum concentration appeared to be 0.5 nM of peptide with a reduction of neutrophil migration up to 60% ($p < 0.001$) compared to the absence of peptide. The same peptide and concentration in the HBMEC cell line showed similar effects ($p<0.05$) although more variability was observed.

In order to characterise the modified version of pCXCL8-1 (pCXCL8-1_{aa}), it was tested in the transwell system before being used *in vivo*. As indicated by the graphs there was a significant reduction of neutrophil migration in both cell lines again between the 0.5 nM – 500 nM range of peptide. These results display a similarity to pCXCL8-1 data confirming that the modifications have not affected the biological activity of the peptide.

The larger pCXCL8-2 peptide was able to reduce neutrophil migration in both cell lines; however, this was less than observed for pCXCL8-1. Using HCMEC/D3 cells at 5 nM of pCXCL8-1, neutrophil migration was reduced by ~60% yet at the same concentration of pCXCL8-2 this reduction was only ~30% compared to the no peptide control; pCXCL8-2 was able to reduce neutrophil migration to the same extent as pCXCL8-1 though at a 10 fold higher concentration. The control peptide had no effect on neutrophil migration and showed significant differences compared to the test peptide. There was some variability between cell lines for this peptide, with significance being reached at 0.5 nM of peptide in the HBMEC cell line compared to a 10 fold higher concentration in the HCMEC/D3 cell line.

pCXCL8-3 significantly reduced neutrophil migration by ~50% at 5, 50 and 500 nM ($p<0.001$) in the HCMEC/D3 cell line, although less than pCXCL8-1 (Supplementary Figure 1a). However, the pCXCL8-4 "dimer" was unable to inhibit CXCL8 induced chemotaxis in the HCMEC/D3 cell line (Supplementary Figure 1b). Due to the complications associated with longer peptides during synthesis, the shorter pCXCL8-1 was chosen in preference as a lead peptide due to the simplicity of its synthesis making it advantageous therapeutically.

The peptide based on the unique C-terminal alpha helix of CXCL12γ showed a stark decrease of neutrophil migration when compared to its no peptide control in the HCMEC/D3 cell line. This peptide reduced neutrophil migration back to baseline levels of ~20% in the HCMEC/D3 cell line at 0.5 nM ($p<0.01$). It demonstrated potency beyond that of others, requiring as little as 0.0005 nM to significantly reduce

neutrophil migration by up to 40%. The peptide also inhibited neutrophil migration significantly more than using the corresponding control peptide at 0.5-50 nM. Similar reduction occurred in the HBMEC cell line although the pattern of inhibition with increasing peptide concentration differed between the two cell types. pCXCL12-1 was assessed for its ability to reduce CXCL8 mediated neutrophil migration across the HCMEC/D3 cell line. The peptide did not significantly reduce neutrophil migration in response to CXCL8 demonstrating some specificity.

pCCL5-3 was unable to reduce monocyte migration across the HCMEC/D3 cell line in response to CCL5 and did not differ compared to its corresponding control peptide. In agreement, the peptide also showed a similar trend in the HBMEC cell line although it did reach significance when compared to CCL5 alone at 5000 nM of peptide ($p = 0.0039$).

Chemokines and peptides based on chemokines bind to human RA synovium.

To examine if the CXCL8 peptide bound to ECs *in situ*, fluorescently labelled pCXCL8-1 was incubated with human RA synovium, and its binding compared to intact CXCL8 labelled with Atto 425. It has been shown previously that CXCL8 binding to HS is upregulated in the ECs of human RA synovium (30). To confirm where the positive staining was observed, a double stain was carried out using Von Willebrand factor to highlight ECs (in red). pCXCL8-1 (Figure 5A) and CXCL8 (Figure 5D) were found to associate with blood vessels, and also with the extracellular matrix (Figure 5B&E). Staining was absent in the negative control sections in the absence of primary antibody, fluorescent CXCL8 or pCXCL8-1 (Figure 5G&H).

The peptide pCXCL8-1 competes with CXCL8 binding

Having confirmed that both the peptide pCXCL8-1 and CXCL8 bind to RA synovium, the question remained whether the peptide competes with CXCL8 for HS binding. Serial sections of human RA synovia were used to assess fluorescent CXCL8 binding (Figure 6A), heparanase treatment prior to CXCL8 binding (Figure 6D) and an equimolar concentration of pCXCL8-1 (0.5 nM) together with CXCL8 (Figure 6G). The representative images seen in Figure 6A and B show that CXCL8 (in green) is associated with ECs stained using Von Willebrand antibody (in red). However, when the synovial sections were pre-treated with heparanase I&III prior to the addition of CXCL8, there was loss of CXCL8 binding (Figure 6D). Additionally, when equimolar concentrations of labelled CXCL8 and unlabelled pCXCL8-1 were added to the sections, a similar loss of CXCL8 binding was observed (Figure 6G). This behaviour is consistent with competitive binding of the peptide pCXCL8-1 and CXCL8 for HS.

The ability of pCXCL8-1 to inhibit binding of CXCL8 to HS was also evaluated using GAG binding plates in an ELISA-like competition assay (Figure 6M). As expected, given its highly positively charged nature, pCXCL8-1 clearly competed with CXCL8. The amount of CXCL8 binding was reduced by all concentrations of pCXCL8-1 and this reached significance at 50 nM ($p<0.05$), reducing the amount of CXCL8 binding by at least 40%. In order to examine this competitive effect on ECs, fluorescently labelled CXCL8 and a range of concentrations of unlabelled pCXCL8-1 were added to HCMEC/D3 cells and the amount of CXCL8 binding was quantified by flow cytometry. As can be seen in Figure 6N, the amount of CXCL8 binding to HCMEC/D3s was reduced in a dose-dependent manor over 0.5-50 nM ($p < 0.001$).

pCXCL8-1aa reduces disease severity and acts as an anti-inflammatory in AIA mouse model

Based on its success at reducing neutrophil migration *in vitro* and its higher affinity for HS than WT CXCL8, pCXCL8-1 could possess anti-inflammatory properties. By competing with chemokines for GAG binding, this peptide could diminish the ability of chemokines to recruit leukocytes to a site of inflammation. Consequently, the anti-inflammatory and therapeutic capability of pCXCL8-1_{aa} was tested in an antigen induced (AIA) mouse model of arthritis. The AIA model shares many histopathological and clinical similarities to human RA (41, 42) making it a useful and relevant model to investigate our peptide. AIA was induced in the right stifle joint of mice and pCXCL8-1_{aa} and corresponding control peptide was injected 6 hours later; when swelling routinely appears in AIA mice and so mimics the early condition in humans.

Histologically AIA was characterised by infiltration of the synovial sub-lining by leukocytes including neutrophils and exudate containing leukocytes in the joint cavity, hyperplasia of the synovial lining and loss of PGs from the articular cartilage (images not shown) as observed in haematoxylin/eosin stained sections (Figure 7A, D and G respectively). These changes did not occur in contralateral knee joints which were injected with PBS instead of mBSA and appeared histologically normal (Figure 7C, F and I). The inflammation, exudate and hyperplasia appeared less severe in pCXCL8-1_{aa} treated mice when compared to the corresponding control peptide (Figure 7B, E and H). To quantitate these changes, the parameters were scored as a measure of disease severity and differences between peptide and control peptide treated mice were evident. At day 7 post injection leukocyte infiltration ($p=0.03$), cellular exudate ($p=0.012$) and hyperplasia ($p=0.009$) were reduced with pCXCL8-1_{aa}.

When all histological parameters were pooled to give an overall arthritic index, as a measure of overall disease severity, pCXCL8-1_{aa} significantly improved the arthritic score when compared to the control peptide at day 7 post injection of mBSA ($p = 0.008$). Differences were not observed at day 3. A similar trend was observed for serum levels of TNFα in AIA mice (Figure 7J). Concentrations of TNFα were reduced at both time points yet reached significance at day 7 post injection of mBSA.

To determine if pCXCL8-1_{aa} could alter neutrophil infiltration into the synovium, the number of these cells were counted in synovial sections (Figure 7K). At 7 days after arthritis induction, pCXCL8-1_{aa} reduced the numbers of neutrophils in the synovium from 5.6 ± 1.1 to 3.1 ± 0.8 with pCXCL8-$1c_{aa}$ ($p<0.05$). At 3 days after arthritis induction there was no significant effect.

Discussion

A recent shift in the interest of the chemokine system as a therapeutic target has focussed on GAGs. Their strong involvement in many disease areas shows potential for the development of glycan targeting therapeutics. In this study, we have contributed to this development by showing that peptides based on chemokines can act as potential anti-inflammatories. Due to the presence of GAG binding domains within the peptides and the undoubted interaction with negatively charged GAGs, a central question was formed. Do the peptides based on chemokines actively compete with chemokines for GAG binding thereby reducing the amount of chemokine being bound and presented; and therefore, do they inhibit chemokine induced leukocyte migration and reduce disease severity? Based on the necessity of chemokine binding to GAGs for exerting biological functions *in vivo*, there is a clear rationale for exploiting the chemokine - GAG interaction. Our peptide design approach takes advantage of the enriched HS-binding domains of chemokines and uses the discrete pocket of highly charged residues as novel anti-inflammatory peptides.

As our approach is intended to keep as close to the natural WT protein, no new GAG binding sites at different locations of the chemokine have been introduced and the peptides exhibit sequence identity with each of the chemokines they are based upon. We intend that this would prevent interference with hydrogen bonding and Van der Waals forces in order to maintain the chemokines in built specificity for the GAG. If maintenance of hydrogen bonding and hydrophobic forces can be achieved, this approach could be a novel and effective way to create efficient and selective GAG antagonists as this is what creates the specificity between chemokines and GAGs (43). Utilising the HS binding domain of chemokines as small chain peptides (lead peptide

is 10 amino acids) is a new approach to combating the chemokine – GAG interaction. Previous approaches have incorporated much more of the chemokine structure with knocked out GPCR activation and have included an unnatural sequence in order to increase the binding affinity of the peptide to GAGs, yet offering increased potential for off-target effects (44). A further advantage of the current novel therapeutic approach is the predictable mechanism by which the peptide works. The peptides based on chemokines interact with GAGs and compete with the WT chemokine for GAG binding. The peptide based on CXCL8 could compete with CXCL8 for binding to HS on binding plates, EC lines and ECs in RA tissue. The binding was associated with EC GAGs as when either ECs or RA tissue were treated with an enzyme to degrade the HS, the binding was visibly reduced. Furthermore, control peptides lacking amino acids that interact with GAGs, such as lysine and arginine, bound significantly less to ECs which agreed with binding isotherm data where the control peptides showed little interaction with HS. This suggests that the interaction of the peptides that do have the lysine and arginine amino acids are in fact interacting with the GAGs present on the EC, and these amino acids are important in the interaction. As GAG expression differs between tissues, especially in inflamed tissue where chemokine binding sites on ECs are up-regulated (40), the peptide could bind to GAGs preferentially in the inflamed tissue and prevent further chemokine induced leukocyte migration.

As a control for our experiments, all peptides were subject to chemotaxis assays whereby the peptide only was placed in the basal chamber and leukocytes were allowed to migrate across an endothelial layer. These peptides did not induce chemotaxis of leukocytes and leukocyte migration remained at baseline (data not

shown). This suggests no functional role of the peptides other than to act as GAG binding antagonists of WT chemokines. Our peptide design approach is clearly dependent upon the knowledge of the GAG-binding site in the target protein which were based on published data. Using these data, we synthesised control peptides which lack the reported HS binding residues and were replaced with a non-charged amino acid. These control peptides were fundamental in distinguishing anti-inflammatory properties of peptides *in vitro* and *in vivo*.

Our peptides were subjected to experiments to assess binding to soluble GAGs. As an initial assessment of peptide interaction with soluble GAGs, they were tested for their binding affinities to HS and DS by IFT. These two GAGs were chosen to show any selectivity by the peptide for particular GAGs. A binding isotherm of WT CXCL8 was measured and peptides based on CXCL8 were compared. In agreement with the literature, WT CXCL8 binds with higher affinity to HS than DS (21, 30). This preference is also apparent for the CCL5 peptide whereas the CXCL12 peptide shows equal preference for HS and DS. In all cases of peptides based on CXCL8, the peptides had a higher affinity than WT CXCL8 for HS and DS. These increased binding affinities of CXCL8 peptides compared to WT CXCL8 shows that the simple peptide design using only identical sequences within chemokines is sufficient to induce a competitive antagonist, perhaps even posing as safe biological molecules based on their natural design. The high fluorescence quenching value (as indicated on the y axis in Figure 2) refers to more efficient fluorescence deactivation and thus to tighter binding of the GAG ligand. This is especially true of pCXCL12-1 where quenching occurs in the first additions of GAG ligand and reaches a quenching value up to 80%. The interaction could be electrostatic in nature however when the salt

level of the solution is increased from physiological levels (137 mM to 400 mM), the affinity of this peptide for HS remains similar (data not shown). This is indicative of a specific peptide – HS interaction. Taken together, these data show a strong affinity of the peptides for GAGs (in the low nM range) making them viable antagonistic molecules. Furthermore, different peptides show selectivity in targeting particular GAGs.

Using an antibody to a HS epitope, we found HS to be present on EC cell lines used in this study, occurring as a mesh-like structure. Confirmation of this expression was achieved with heparanases; when the ECs were incubated with both heparanase I and III, the expression of HS was reduced to background. HS on ECs has been widely reported to bind, concentrate and present chemokines to leukocytes during extravasation (24, 27, 34, 45). Indeed, we have shown that CXCL8 binding to ECs is reduced when the cells are treated with heparanases alongside the fact that our control peptide pCXCL8-1c shows little interaction with ECs corroborates HS as a key player in chemokine activity. The implications of this are clearly shown in

Figure 3E where neutrophil transmigration through an endothelial monolayer that has been pre-treated with heparanases is vastly reduced.

Using our peptides based on chemokines, we were able to show a reduction of leukocyte migration in a cell culture model of inflammation. By placing chemokine in the basal chamber, the chemokine would be transcytosed or diffuse to the EC surface thereby creating a chemotactic gradient for the leukocytes placed into the apical chamber (27). The peptides were tested in two separate cell lines to confirm results. Peptides based on CXCL8 (apart from pCXCL8-4) were able to reduce leukocyte transendothelial migration. Interestingly, in agreement with IFT binding affinity data, the smaller pCXCL8-1 peptide with 3 HS binding sites showed increased efficacy and was most efficacious in the low nanomolar range unlike pCXCL8-2 which has 4 HS binding domains and required a higher concentration to elicit similar results. pCXCL8-3 could inhibit CXCL8 induced neutrophil migration from 0.5nM to 5000nM however the optimum concentration was 500nM and therefore much higher than pCXCL8-1. Conversely pCXCL8-4 showed no anti-chemotactic ability *in vitro*. Our results suggest that the two lysine and one arginine residues in the final 10 amino acids of the C-terminus of CXCL8 are especially important in its functional interaction with HS in terms of driving leukocyte migration. In addition, there is specificity in the interaction since adding the CXCL12γ peptide instead of CXCL8 peptide had no inhibitory effect on CXCL8 driven neutrophil migration, despite the increased affinity of this peptide for HS as shown by IFT. Therefore, the CXCL8 peptide binding site on HS may be different from that of the CXCL12γ peptide.

Our peptide utilising the C-terminus of CXCL12γ was highly potent and showed a marked decrease in neutrophil transendothelial migration compared to a control. However, unlike some of the other peptides, a difference between cell lines was observed. In addition, the pCXCL12-1 peptide shows specificity in action as it was unable to inhibit CXCL8 induced neutrophil migration. The peptide based on CCL5 showed promising IFT data with a high affinity for HS however this did not translate into success *in vitro*. pCCL5-3 was unable to exhibit an anti-chemotactic effect on mononuclear cells using HCMEC/D3 cells and a very small effect using HMBECs. This could be due to a number of different reasons, one being the very small size of the peptide (Mr = 773) or perhaps that mononuclear cell migration is through an alternative mechanism. As we've shown, heparanase treatment does not have as extensive a reduction of CCL5 mediated leukocyte migration as it does on CXCL8 migration. This suggests a role for perhaps another GAG or a molecule like the Duffy antigen receptor for chemokines (DARC) whose role is less clear in chemokine presentation to leukocytes.

The results show that CXCL8 binds to RA synovium, as does the peptide pCXCL8-1. The pattern of binding was similar to that of HS staining (30), being associated with blood vessels, and some was observed in the extracellular matrix. Studies have previously shown similar CXCL8 binding which was attributable to the presence of HSPGs on ECs and the extracellular matrix (30). It was investigated if pCXCL8-1 could compete for CXCL8 binding to GAGs in cultured ECs and RA synovia. We clearly demonstrated a reduction in CXCL8 binding in the presence of peptide, moreover the binding is HS dependent as the use of heparanases also reduces CXCL8

binding. In addition, the competitive nature of pCXCL8-1 was shown in HS binding plates in an ELISA like assay, despite the varying concentrations used which was necessitated by the different techniques.

Following effects *in vitro* and *in situ*, our lead peptide pCXCL8-1 was evaluated in an AIA murine model after modifications to render it less susceptible to proteolytic degradation (pCXCL8-1_{aa}). Previous work has validated this model as suitable to test therapeutic agents that interfere with the CXCL8 axis (46) as the model's pathology is driven by the mouse functional homologue of CXCL8. We have shown that pCXCL8-1_{aa} was able to reduce several parameters involved in arthritis, significantly reducing the overall arthritic score as a measure of disease severity. The reduction was characterised by reduced leukocyte infiltrate into the synovium and joint space, particularly including neutrophils. Neutrophils are considered influential cells in the development of inflammatory joint disease, as supported by several studies involving experimental models of arthritis. Neutrophils are found in high numbers within the human rheumatoid joint where they play a significant role in inflicting damage to the tissue, bone and cartilage by secretion of proteases and toxic oxygen species, as well as driving further inflammation through secretion of cytokines, chemokines and prostaglandins (47). This suggests that targeting CXCL8 driven neutrophil extravasation with CXCL8 peptides is successful and beneficial. Furthermore, it is possible that inhibiting a mainly neutrophil attracting chemokine (CXCL8) can have a direct or indirect effect on other cells and pathological features of RA. Hyperplasia of the synovial lining layer occurs in RA and is proposed to occur via the recruitment of monocytes in the sub-lining blood vessels which then migrate and insert into the lining layer (48, 49). Here, the monocytes are activated and differentiate into

macrophages and undergo hyperplasia. Monocyte adherence to the endothelium is increased by the presence of CXCL8 and so by reducing the amount of CXCL8 presentation, the peptide may be able to reduce monocyte recruitment and hence hyperplasia of the lining layer. By reducing neutrophil recruitment, it is possible that recruitment of other cell types via reduced chemokine and cytokine production such as TNFα is also reduced. Here we show that pCXCL8-1_{aa} reduces the levels of TNFα in the circulation of AIA mice. TNFα is a central cytokine involved in inflammation and tissue degradation in RA and blocking this cytokine is the major current therapy for the disease. The decrease in TNFα levels suggest that administration of pCXCL8-1 can reduce systemic inflammation, which is a feature of RA, in addition to having local effects in the joint.

In summary, GAGs are an abundant class of highly sulphated polysaccharides that are known to drive and control protein activity by interacting with basic amino acids on the target protein. We have targeted this functional interaction as a potential way of antagonising the target protein's pathological role. Chemokines are clearly beneficial in the battle against infectious organisms and during wound healing after tissue injury, yet excessive and on-going chemokine expression has been associated with inflammatory disorders, characterised by an inappropriate increase in leukocyte infiltration (50). The chemokine system, therefore, seems an attractive target for modulating such diseases. Interestingly, other species have already manipulated the chemokine system to their own benefit. For example, viruses and ticks have successfully used this strategy to evade the host's immune system (51) by producing homologues of chemokines and chemokine receptors thereby altering and controlling their activity. The chemokine system has been the subject of therapeutic interest for

many years with previous strategies focussing on chemokine receptor antagonists (52). Unfortunately, the labours of this train of thought have been largely unsuccessful in clinical trials. More recent strategies have employed the use of the chemokine - GAG interaction. The recently developed CellJammer approach seeks to develop mutant chemokines with increased GAG binding affinity and knocked out GPCR function, thus creating an antagonist for WT chemokines. This approach has been successfully applied to create antagonists for CXCL8 and CCL2 (46, 53). CXCL8 and CCL2 based "decoy" molecules were shown to moderate inflammation in various mouse models such as ischemia/reperfusion, AIA, renal allograft rejection and experimental autoimmune uveitis. Most recently, a C-terminal peptide based on CXCL9 was shown to inhibit neutrophil extravasation and monosodium urate crystal induced gout in mice (54). The amounting evidence in support for the chemokine - GAG strategy is compelling. Our approach, although similar to these recent studies, is a simplified and more natural design. Our lead peptide is a mere 10 amino acids in length making it a quick, cheap and easy molecule to synthesise therapeutically. Not only this but the data gathered confirms the chemokine - GAG interaction as a biologically relevant target.

Acknowledgements

The authors would like to thank Dr Andrew Herman and the flow cytometry department of Bristol University including the loan of Atto 425. They would also like to thank the PPR Ltd team of peptide chemists for all their assistance in synthesis and analytical techniques and the team of AJK at the University of Graz, Austria for their help with IFT experiments.

References

1. Vestweber, D. 2015. How leukocytes cross the vascular endothelium. In *Nat Rev Immunol*, England. 692-704.
2. Phillipson, M., B. Heit, P. Colarusso, L. Liu, C. M. Ballantyne, and P. Kubes. 2006. Intraluminal crawling of neutrophils to emigration sites: a molecularly distinct process from adhesion in the recruitment cascade. *J Exp Med* 203: 2569-2575.
3. Griffith, J. W., C. L. Sokol, and A. D. Luster. 2014. Chemokines and chemokine receptors: positioning cells for host defense and immunity. *Annu Rev Immunol* 32: 659-702.
4. Kufareva, I., C. L. Salanga, and T. M. Handel. 2015. Chemokine and chemokine receptor structure and interactions: implications for therapeutic strategies. *Immunol Cell Biol* 93: 372-383.
5. Lau, E. K., S. Allen, A. R. Hsu, and T. M. Handel. 2004. Chemokine-receptor interactions: GPCRs, glycosaminoglycans and viral chemokine binding proteins. In *Adv Protein Chem*, United States. 351-391.
6. Clark-Lewis, I., K. S. Kim, K. Rajarathnam, J. H. Gong, B. Dewald, B. Moser, M. Baggiolini, and B. D. Sykes. 1995. Structure-activity relationships of chemokines. *J Leukoc Biol* 57: 703-711.
7. Proudfoot, A. E., C. A. Power, A. J. Hoogewerf, M. O. Montjovent, F. Borlat, R. E. Offord, and T. N. Wells. 1996. Extension of recombinant human RANTES by the retention of the initiating methionine produces a potent antagonist. *J Biol Chem* 271: 2599-2603.
8. Proudfoot, A. E., P. Bonvin, and C. A. Power. 2015. Targeting chemokines: Pathogens can, why can't we? In *Cytokine*. 2015 Elsevier Ltd, England. 259-267.
9. Bardi, G., M. Lipp, M. Baggiolini, and P. Loetscher. 2001. The T cell chemokine receptor CCR7 is internalized on stimulation with ELC, but not with SLC. In *Eur J Immunol*, Germany. 3291-3297.
10. Handel, T. M., Z. Johnson, S. E. Crown, E. K. Lau, and A. E. Proudfoot. 2005. Regulation of protein function by glycosaminoglycans--as exemplified by chemokines. *Annu Rev Biochem* 74: 385-410.
11. Capila, I., and R. J. Linhardt. 2002. Heparin-protein interactions. In *Angew Chem Int Ed Engl*, Germany. 391-412.
12. Sugahara, K., T. Mikami, T. Uyama, S. Mizuguchi, K. Nomura, and H. Kitagawa. 2003. Recent advances in the structural biology of chondroitin sulfate and dermatan sulfate. In *Curr Opin Struct Biol*, England. 612-620.
13. Esko, J. D., and S. B. Selleck. 2002. Order out of chaos: assembly of ligand binding sites in heparan sulfate. In *Annu Rev Biochem*, United States. 435-471.
14. Parish, C. R. 2006. The role of heparan sulphate in inflammation. In *Nat Rev Immunol*, England. 633-643.
15. Ihrcke, N. S., L. E. Wrenshall, B. J. Lindman, and J. L. Platt. 1993. Role of heparan sulfate in immune system-blood vessel interactions. In *Immunol Today*, England. 500-505.
16. Sadir, R., A. Imberty, F. Baleux, and H. Lortat-Jacob. 2004. Heparan sulfate/heparin oligosaccharides protect stromal cell-derived factor-1 (SDF-1)/CXCL12 against proteolysis induced by CD26/dipeptidyl peptidase IV. In *J Biol Chem*, United States. 43854-43860.

17. Johnson, Z., M. H. Kosco-Vilbois, S. Herren, R. Cirillo, V. Muzio, P. Zaratin, M. Carbonatto, M. Mack, A. Smailbegovic, M. Rose, R. Lever, C. Page, T. N. Wells, and A. E. Proudfoot. 2004. Interference with heparin binding and oligomerization creates a novel anti-inflammatory strategy targeting the chemokine system. In *J Immunol*, United States. 5776-5785.
18. Middleton, J., A. M. Patterson, L. Gardner, C. Schmutz, and B. A. Ashton. 2002. Leukocyte extravasation: chemokine transport and presentation by the endothelium. In *Blood*, United States. 3853-3860.
19. Ali, S., S. J. Fritchley, B. T. Chaffey, and J. A. Kirby. 2002. Contribution of the putative heparan sulfate-binding motif BBXB of RANTES to transendothelial migration. *Glycobiology* 12: 535-543.
20. Proudfoot, A. E., S. Fritchley, F. Borlat, J. P. Shaw, F. Vilbois, C. Zwahlen, A. Trkola, D. Marchant, P. R. Clapham, and T. N. Wells. 2001. The BBXB motif of RANTES is the principal site for heparin binding and controls receptor selectivity. In *J Biol Chem*, United States. 10620-10626.
21. Kuschert, G. S., F. Coulin, C. A. Power, A. E. Proudfoot, R. E. Hubbard, A. J. Hoogewerf, and T. N. Wells. 1999. Glycosaminoglycans interact selectively with chemokines and modulate receptor binding and cellular responses. In *Biochemistry*, United States. 12959-12968.
22. Dyer, D. P., J. M. Thomson, A. Hermant, T. A. Jowitt, T. M. Handel, A. E. Proudfoot, A. J. Day, and C. M. Milner. 2014. TSG-6 inhibits neutrophil migration via direct interaction with the chemokine CXCL8. *J Immunol* 192: 2177-2185.
23. Kumar, A. V., S. K. Katakam, A. K. Urbanowitz, and M. Gotte. 2015. Heparan sulphate as a regulator of leukocyte recruitment in inflammation. In *Curr Protein Pept Sci*, Netherlands. 77-86.
24. Proudfoot, A. E., T. M. Handel, Z. Johnson, E. K. Lau, P. LiWang, I. Clark-Lewis, F. Borlat, T. N. Wells, and M. H. Kosco-Vilbois. 2003. Glycosaminoglycan binding and oligomerization are essential for the in vivo activity of certain chemokines. *Proc Natl Acad Sci U S A* 100: 1885-1890.
25. Wang, L., M. Fuster, P. Sriramarao, and J. D. Esko. 2005. Endothelial heparan sulfate deficiency impairs L-selectin- and chemokine-mediated neutrophil trafficking during inflammatory responses. In *Nat Immunol*, United States. 902-910.
26. Webb, L. M., M. U. Ehrengruber, I. Clark-Lewis, M. Baggiolini, and A. Rot. 1993. Binding to heparan sulfate or heparin enhances neutrophil responses to interleukin 8. *Proc Natl Acad Sci U S A* 90: 7158-7162.
27. Middleton, J., S. Neil, J. Wintle, I. Clark-Lewis, H. Moore, C. Lam, M. Auer, E. Hub, and A. Rot. 1997. Transcytosis and surface presentation of IL-8 by venular endothelial cells. In *Cell*, United States. 385-395.
28. Lensen, J. F., A. L. Rops, T. J. Wijnhoven, T. Hafmans, W. F. Feitz, E. Oosterwijk, B. Banas, R. J. Bindels, L. P. van den Heuvel, J. van der Vlag, J. H. Berden, and T. H. van Kuppevelt. 2005. Localization and functional characterization of glycosaminoglycan domains in the normal human kidney as revealed by phage display-derived single chain antibodies. In *J Am Soc Nephrol*, United States. 1279-1288.
29. Sasisekharan, R., Z. Shriver, G. Venkataraman, and U. Narayanasami. 2002. Roles of heparan-sulphate glycosaminoglycans in cancer. In *Nat Rev Cancer*, England. 521-528.

30. Patterson, A. M., L. Gardner, J. Shaw, G. David, E. Loreau, L. Aguilar, B. A. Ashton, and J. Middleton. 2005. Induction of a CXCL8 binding site on endothelial syndecan-3 in rheumatoid synovium. *Arthritis Rheum* 52: 2331-2342.
31. Kehoe, O., N. Kalia, S. King, A. Eustace, C. Boyes, O. Reizes, A. Williams, A. Patterson, and J. Middleton. 2014. Syndecan-3 is selectively pro-inflammatory in the joint and contributes to antigen-induced arthritis in mice. *Arthritis Res Ther* 16: R148.
32. Marquezini, M. V., C. M. Strunz, L. A. Dallan, and O. M. Toledo. 1995. Glycosaminoglycan distribution in atherosclerotic saphenous vein grafts. *Cardiology* 86: 143-146.
33. Murch, S. H., T. T. MacDonald, J. A. Walker-Smith, M. Levin, P. Lionetti, and N. J. Klein. 1993. Disruption of sulphated glycosaminoglycans in intestinal inflammation. In *Lancet*, England. 711-714.
34. Hoogewerf, A. J., G. S. Kuschert, A. E. Proudfoot, F. Borlat, I. Clark-Lewis, C. A. Power, and T. N. Wells. 1997. Glycosaminoglycans mediate cell surface oligomerization of chemokines. In *Biochemistry*, United States. 13570-13578.
35. Kuschert, G. S., A. J. Hoogewerf, A. E. Proudfoot, C. W. Chung, R. M. Cooke, R. E. Hubbard, T. N. Wells, and P. N. Sanderson. 1998. Identification of a glycosaminoglycan binding surface on human interleukin-8. In *Biochemistry*, United States. 11193-11201.
36. Rueda, P., K. Balabanian, B. Lagane, I. Staropoli, K. Chow, A. Levoye, C. Laguri, R. Sadir, T. Delaunay, E. Izquierdo, J. L. Pablos, E. Lendinez, A. Caruz, D. Franco, F. Baleux, H. Lortat-Jacob, and F. Arenzana-Seisdedos. 2008. The CXCL12gamma chemokine displays unprecedented structural and functional properties that make it a paradigm of chemoattractant proteins. *PLoS One* 3: e2543.
37. Weksler, B. B., E. A. Subileau, N. Perriere, P. Charneau, K. Holloway, M. Leveque, H. Tricoire-Leignel, A. Nicotra, S. Bourdoulous, P. Turowski, D. K. Male, F. Roux, J. Greenwood, I. A. Romero, and P. O. Couraud. 2005. Blood-brain barrier-specific properties of a human adult brain endothelial cell line. In *FASEB J*, United States. 1872-1874.
38. Weksler, B., I. A. Romero, and P. O. Couraud. 2013. The hCMEC/D3 cell line as a model of the human blood brain barrier. *Fluids Barriers CNS* 10: 16.
39. Whittall, C., O. Kehoe, S. King, A. Rot, A. Patterson, and J. Middleton. 2013. A chemokine self-presentation mechanism involving formation of endothelial surface microstructures. *J Immunol* 190: 1725-1736.
40. Patterson, A. M., A. Cartwright, G. David, O. Fitzgerald, B. Bresnihan, B. A. Ashton, and J. Middleton. 2008. Differential expression of syndecans and glypicans in chronically inflamed synovium. *Ann Rheum Dis* 67: 592-601.
41. Nowell, M. A., P. J. Richards, S. Horiuchi, N. Yamamoto, S. Rose-John, N. Topley, A. S. Williams, and S. A. Jones. 2003. Soluble IL-6 receptor governs IL-6 activity in experimental arthritis: blockade of arthritis severity by soluble glycoprotein 130. *J Immunol* 171: 3202-3209.
42. Brackertz, D., G. F. Mitchell, and I. R. Mackay. 1977. Antigen-induced arthritis in mice. I. Induction of arthritis in various strains of mice. *Arthritis Rheum* 20: 841-850.
43. Adage, T., A. M. Piccinini, A. Falsone, M. Trinker, J. Robinson, B. Gesslbauer, and A. J. Kungl. 2012. Structure-based design of decoy

chemokines as a way to explore the pharmacological potential of glycosaminoglycans. *Br J Pharmacol* 167: 1195-1205.

44. Gschwandtner, M., A. M. Piccinini, T. Gerlza, T. Adage, and A. J. Kungl. 2016. Interfering with the CCL2-glycosaminoglycan axis as a potential approach to modulate neuroinflammation. In *Neurosci Lett*. 2016 Elsevier Ireland Ltd, Ireland. 164-173.
45. Ali, S., H. Robertson, J. H. Wain, J. D. Isaacs, G. Malik, and J. A. Kirby. 2005. A non-glycosaminoglycan-binding variant of CC chemokine ligand 7 (monocyte chemoattractant protein-3) antagonizes chemokine-mediated inflammation. In *J Immunol*, United States. 1257-1266.
46. Falsone, A., V. Wabitsch, E. Geretti, H. Potzinger, T. Gerlza, J. Robinson, T. Adage, M. M. Teixeira, and A. J. Kungl. 2013. Designing CXCL8-based decoy proteins with strong anti-inflammatory activity in vivo. *Biosci Rep* 33.
47. Wright, H. L., R. J. Moots, R. C. Bucknall, and S. W. Edwards. 2010. Neutrophil function in inflammation and inflammatory diseases. In *Rheumatology (Oxford)*, England. 1618-1631.
48. Patterson, A. M., H. Siddall, G. Chamberlain, L. Gardner, and J. Middleton. 2002. Expression of the duffy antigen/receptor for chemokines (DARC) by the inflamed synovial endothelium. *J Pathol* 197: 108-116.
49. Patterson, A. M., C. Schmutz, S. Davis, L. Gardner, B. A. Ashton, and J. Middleton. 2002. Differential binding of chemokines to macrophages and neutrophils in the human inflamed synovium. *Arthritis Res* 4: 209-214.
50. Szekanecz, Z., A. Vegvari, Z. Szabo, and A. E. Koch. 2010. Chemokines and chemokine receptors in arthritis. *Front Biosci (Schol Ed)* 2: 153-167.
51. Alcami, A., and S. A. Lira. 2010. Modulation of chemokine activity by viruses. In *Curr Opin Immunol*. 2010 Elsevier Ltd, England. 482-487.
52. Allegretti, M., M. C. Cesta, A. Garin, and A. E. Proudfoot. 2012. Current status of chemokine receptor inhibitors in development. In *Immunol Lett*. 2012 Elsevier B.V, Netherlands. 68-78.
53. Bedke, J., P. J. Nelson, E. Kiss, N. Muenchmeier, A. Rek, C. L. Behnes, N. Gretz, A. J. Kungl, and H. J. Grone. 2010. A novel CXCL8 protein-based antagonist in acute experimental renal allograft damage. In *Mol Immunol*. 2009 Elsevier Ltd, England. 1047-1057.
54. Vanheule, V., R. Janssens, D. Boff, N. Kitic, N. Berghmans, I. Ronsse, A. J. Kungl, F. A. Amaral, M. M. Teixeira, J. Van Damme, P. Proost, and A. Mortier. 2015. The Positively Charged COOH-terminal Glycosaminoglycan-binding CXCL9(74-103) Peptide Inhibits CXCL8-induced Neutrophil Extravasation and Monosodium Urate Crystal-induced Gout in Mice. *J Biol Chem* 290: 21292-21304.

Tables

Table 1: Peptides and control peptides showing sequences and molecular weight.

Peptide	Sequence	Molecular Weight
pCXCL8-1	^{63}EKFLKRAENS^{72}	1220
pCXCL8-1c	^{63}EAFLGSAENS^{72}	1024
pCXCL8-1$_{aa}$	Ac-^{63}EKFLKRAENS^{72}-NH_2	1262
pCXCL8-1c$_{aa}$	Ac-^{63}EAFLGSAENS^{72}-NH_2	1065
pCXCL8-2	^{58}VQRVVE KFLKRAENS^{72}	1803
pCXCL8-2c	^{58}VQAVVE AFLGSAENS^{72}	1520
pCXCL8-3	^{20}KFIK ELRVIESGPH CANTEIIVKL SDGRELCLDP KENWVQRVVE KFLKRAENS^{72}	6167
pCXCL8-4	^{55}ENWVQRVVE KFLKRAENS^{72} GSGSG ^{55}ENWVQRVVE KFLKRAENS^{72}	4792
pCCL5-1	^{44}RKNR^{47}	572
pCCL5-2	^{43}TRKNR^{47}	673
pCCL5-3	^{42}VTRKNR^{47}	773
pCCL5-3c	^{42}VTGSGS^{47}	506
pCXCL12-1	^{68}GRREEKVGKKE KIGKKKRQKK RKAAQKRKN^{98}	3620
pCXCL12-1c	^{68}GRREEKVGGSG SIGGSGSQGS GSAAQKRKN^{98}	2889

aa = amidated & acetylated

c = control

p = peptide

Table 2: Affinity of peptides for HS and DS

Peptide/Protein	**Heparan Sulphate (HS)**		**Dermatan Sulphate (DS)**	
	Kd (nM)	± SD	Kd (nM)	± SD
WT *f*CXCL8	128	5	170	13
*f*pCXCL8-1	15	3	44	3
*f*pCXCL8-2	61	5	52	3
*f*pCXCL8-1$_{aa}$	65	4	45	2
*f*pCCL5-3	8	1	148	7
*f*pCXCL12-1	2	0.5	3	0.2

aa = C-terminal amidation
f = FITC labelled
p = peptide
WT = wildtype

Table 3: Scores from each histological parameter at day 3 and day 7 of AIA.

Timepoint	Peptide	Hyperplasia	Synovial Infiltrate	Exudate	Cartilage depletion	Arthritic Index
Day 3	pCXCL8-1$_{aa}$	2 ± 0.3	2.9 ± 0.5	2.1 ± 0.2	1.2 ± 0.5	8.2 ± 1.3
	pCXCL8-1c$_{aa}$	2 ± 0.4	3.3 ± 0.5	2.1 ± 0.5	0.1 ± 0.1	7.4 ± 0.9
Day 7	pCXCL8-1$_{aa}$	1.4 ± 0.2**	1.3 ± 0.4*	0.4 ± 0.2*	0.8 ± 0.5	3.9 ± 0.9**
	pCXCL8-1c$_{aa}$	2.6 ± 0.3	3.2 ± 0.6	1.4 ± 0.2	1.5 ± 0.5	8.7 ± 1.0

*p<0.05, **p<0.01 compared to control peptide.

aa = amidated & acetylated

c = control

p = peptide

Figure Legends

Figure 1: Modelling peptides based on chemokines

(A) Wildtype CXCL8 (B) C-terminal peptides (pCXCL8-1 and -2) indicated in blue where -1 is dark blue and -2 is the longer peptide indicated by two blue shades, (C) longer peptide (pCXCL8-3) including all known HS binding sites as shown by the green and purple structures and the yellow highlighting the N-terminal residues which were removed, (D) both C-terminal alpha helices (pCXCL8-4) linked together by a pre-modelled linker to form a "dimer". (E) Wildtype CCL5. (F) Indicated are peptides based on the 40s loop of CCL5 (pCCL5-1 / -2 / -3) with pCCL5-3 being the longest indicated by two blue shades and grey, pCCL5-2 two blue shades and pCCL5-1 dark blue. (G) Wildtype CXCL12γ. (H) C-terminal peptide (pCXCL12-1) indicated in blue. Carbon atoms are seen in green and pink where each represents the monomeric unit, oxygen in red, nitrogen in blue and sulphur in yellow (A, E and G). Structures are shown as dimers. Please note that CXCL8 and CXCL12 peptides are not helical in structure but are based on the helical sequences present in the wildtype chemokine.

Figure 2: Binding isotherms of peptide interactions with GAGs

Isothermal fluorescent titration binding of peptide is shown to either HS (black) or DS (red). Control peptide interaction with HS is shown in green. On the y-axis, the relative change in fluorescence intensity following ligand addition is displayed: dF = F (fluorescence emission at a certain GAG concentration) − F 0 (fluorescence emission in the absence of ligand). K_d based on line of best fit taken from the mean of three separate experiments ± SD.

Figure 3: The role of endothelial HS in leukocyte transendothelial migration and chemokine/peptide binding.

HCMEC/D3s were stained with anti-HS 10e4 antibody. (A) HS expression as indicated by mesh-work like pattern, (B) plus DAPI. (C) ECs were pre-treated with heparanase I&III, (D) plus DAPI. (E) Neutrophil transendothelial migration after EC treatment with heparanase I&III in response to CXCL8 stimulus, (F) mononuclear transendothelial migration after EC treatment with heparanase I&III in response to CCL5 stimulus. HCMEC/D3s were pre-treated with heparanase I&III and the ability of chemokine or peptide to bind to the cells was assessed by detection of a fluorescent signal by flow cytometry. (G) CXCL8 binding, (H) pCXCL8-1 binding. (E-H) Data shown are means **(**n=3) ± SE. **p<0.01, ***p<0.001, ****p<0.0001. Scale bar = 20μm for all images. Percentage migration is calculated from the total number of cells added.

Figure 4: Anti-chemotactic effects of peptides on leukocyte transendothelial migration.

Anti-chemotactic ability of peptides was tested in HBMEC and HCMEC/D3 cell lines. On the y axis percentage of transendothelial migration in response to increasing concentration of peptide (nM) on the x axis. Indicated (±) is the presence of 100 ng/ml chemokine. The effect of the peptide (black) is compared to a control peptide (white). For CXCL8 and CXCL12γ peptides neutrophils were used and mononuclear cells for the CCL5 peptide. Data shown are mean transendothelial migration ± SE (n=3). *$p<0.05$, **$p<0.01$, ***$p<0.001$ compared to chemokine alone in absence of peptide, §$p<0.05$, §§$p<0.01$, §§§$p<0.001$, §§§§$p<0.0001$. Percentage migration is calculated from the total number of cells added.

Figure 5: Peptide pCXCL8-1 and CXCL8s interact with ECs in human RA synovium.

Representative immunofluorescence images of human RA synovium. Von Willebrand factor staining is in red highlighting ECs and green represents either pCXCL8-1 or CXCL8 positive staining. (A) pCXCL8-1 binding, (B) Von Willebrand factor, (C) DAPI. (D) CXCL8 binding, (E) Von Willebrand factor, (F) DAPI. (G) Negative control with no pCXCL8-1 or CXCL8, (H) no Von Willebrand factor, (I) DAPI. Arrows indicate positive pCXCL8-1 or CXCL8 staining of blood vessels and in the extracellular matrix. Scale bar = 50 μm for each image.

Figure 6: The peptide pCXCL8-1 competes with CXCL8 binding.

Serial sections of human RA synovium were cut and incubated with fluorescent CXCL8 (5 µg/ml/0.5 nM) in order to assess binding competition by unlabelled pCXCL8-1 (0.5 nM). (A) CXCL8 binding only, (B) Von Willebrand factor, (C) DAPI. (D) CXCL8 binding after treatment with heparanase I&III. (G) CXCL8 binding with the addition of equimolar pCXCL8-1. J-L is the negative control in the absence of fluorescent CXCL8, pCXCL8-1 or Von Willebrand antibody. Scale bar = 50 µm for each image. (M) To assess whether pCXCL8-1 could compete with CXCL8 for HS binding, GAG binding plates in an ELISA-like assay were used to evaluate a reduction of CXCL8 binding with a dose dependent increase of pCXCL8-1. (N) In a similar experiment, HCMEC/D3 cells were treated with Atto 425 labelled CXCL8, an increasing dose of pCXCL8-1 was added and the CXCL8 signal detected by flow cytometry. Data shown are means ± SE (n=3). *P<0.05, ***p<0.001 compared to the negative control in the absence of peptide.

Figure 7: Murine antigen induced arthritis.

Arthritis was induced by intra-articular injection of methylated BSA in the right knee (stifle) joint followed by intra-articular injection of 5μg pCXCL8-1_{aa} or pCXCL8-$1c_{aa}$ 6 hours later. For a non-arthritic control, PBS was injected into the left knee joint. (A-I) Representative histological images stained with H&E. (A) pCXCL8-$1c_{aa}$ treated joint showing synovial infiltrate (as indicated by *), inset shows detail of cell infiltrate containing neutrophil population (scale bar = 20 μm), (B) pCXCL8-1_{aa}, (C) PBS control. Images showing synovial exudate (as indicated by arrow) in (D) pCXCL8-$1c_{aa}$, (E) pCXCL8-1_{aa}, (F) PBS control; Scale bar = 200 μm in each image. Images showing synovial hyperplasia (as indicated by arrow) in (G) pCXCL8-$1c_{aa}$, (H) pCXCL8-1_{aa}, (I) PBS control; Scale bar = 40 μm in each image. (J) Serum concentrations of TNFα were analysed by ELISA. (K) The effect of pCXCL8-1_{aa} on neutrophil infiltration in the synovium in comparison to pCXCL8-$1c_{aa}$. Neutrophils were quantified by counting cell numbers in 5 random fields of view in H&E sections at x1000 magnification. Data shown are means ± SE (n=5 mice), *$p<0.05$.

Supplementary Figure 1: Anti-chemotactic effects of pCXCL8-3 and pCXCL8-4 on leukocyte transendothelial migration.

Anti-chemotactic ability of peptides was tested in HCMEC/D3 cells. On the y axis percentage of neutrophil transendothelial migration in response to increasing concentration of peptide (nM) on the x axis. Indicated (±) is the presence of 100 ng/ml chemokine. Data shown are mean transendothelial migration ± SE (n=3). **p<0.01, ***p<0.001 compared to chemokine alone in absence of peptide, §§p<0.01, §§§p<0.001. Percentage migration is calculated from the total number of cells added.

Figures

Figure 1

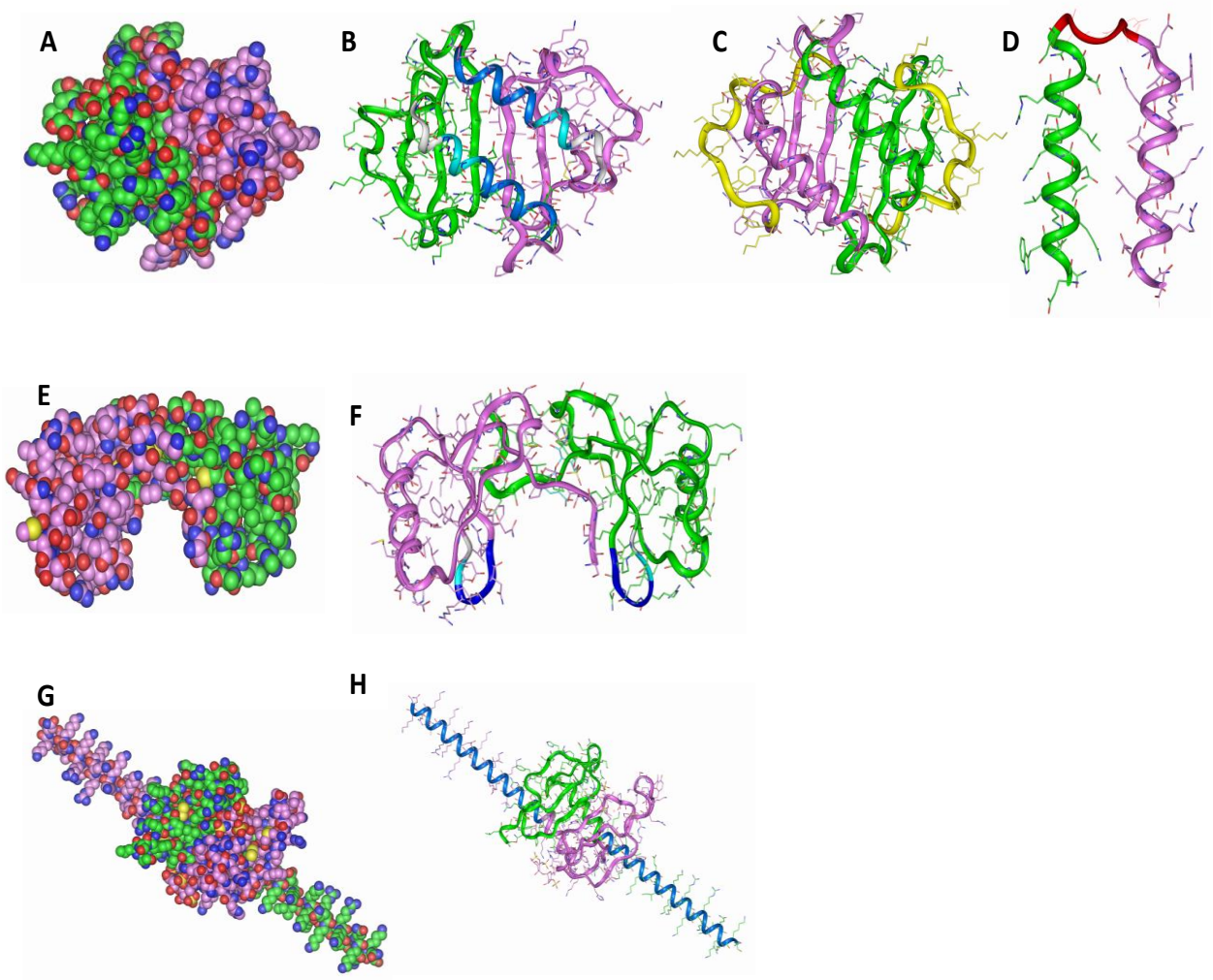

Figure 2

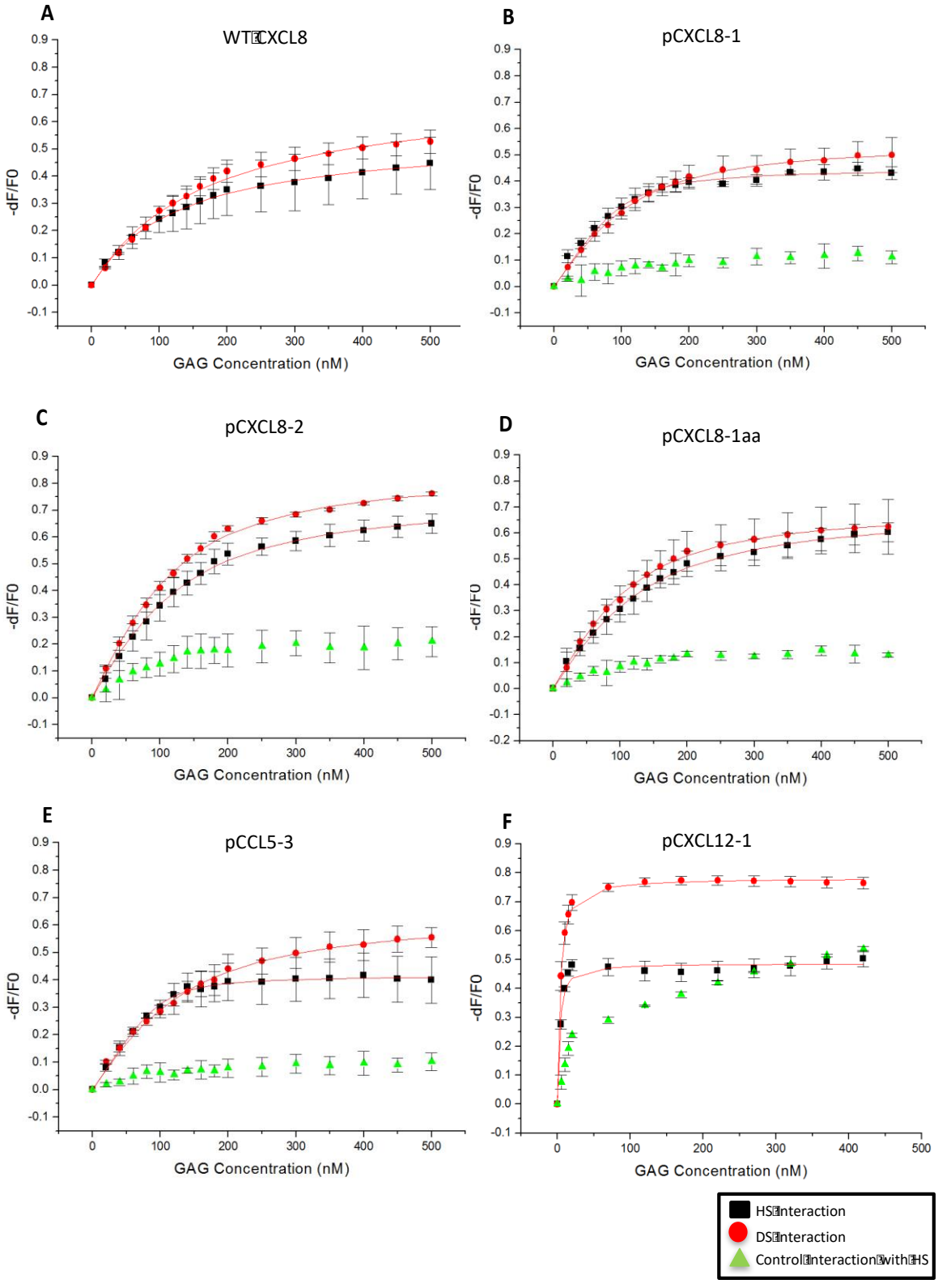
A
WT CXCL8
B
pCXCL8-1
C
pCXCL8-2
D
pCXCL8-1aa
E
pCCL5-3
F
pCXCL12-1
-dF/F0
GAG Concentration (nM)
HS Interaction
DS Interaction
Control Interaction with HS

Figure 3

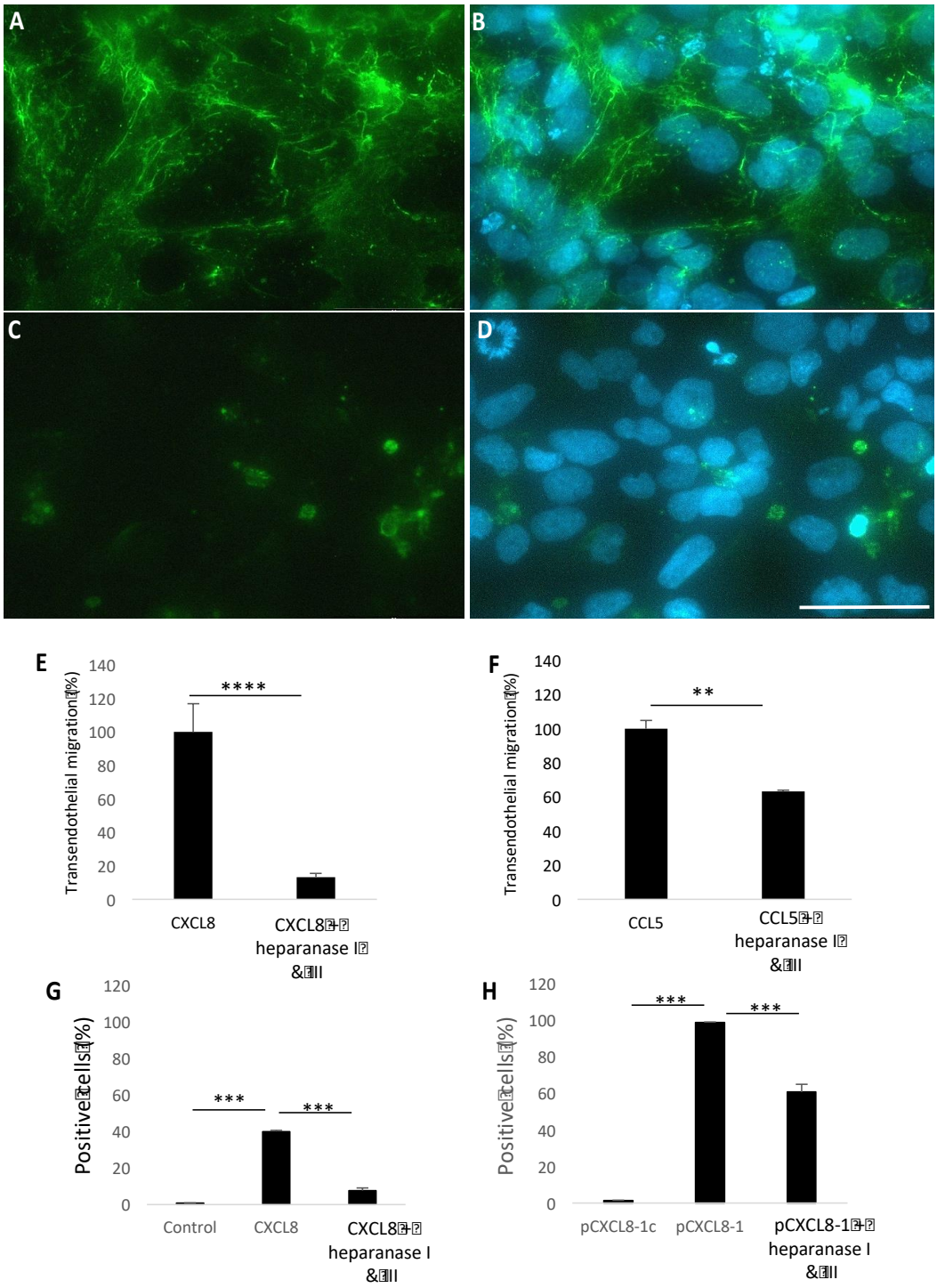
A
B
C
D
E
Transendothelial migration (%)
140
120
100
80
60
40
20
0
****
CXCL8
CXCL8 + heparanase I & III
F
Transendothelial migration (%)
**
CCL5
CCL5 + heparanase I & III
G
Positive cells (%)
***
***
Control
CXCL8
CXCL8 + heparanase I & III
H
Positive cells (%)
***
***
pCXCL8-1c
pCXCL8-1
pCXCL8-1 + heparanase I & III

Figure 4

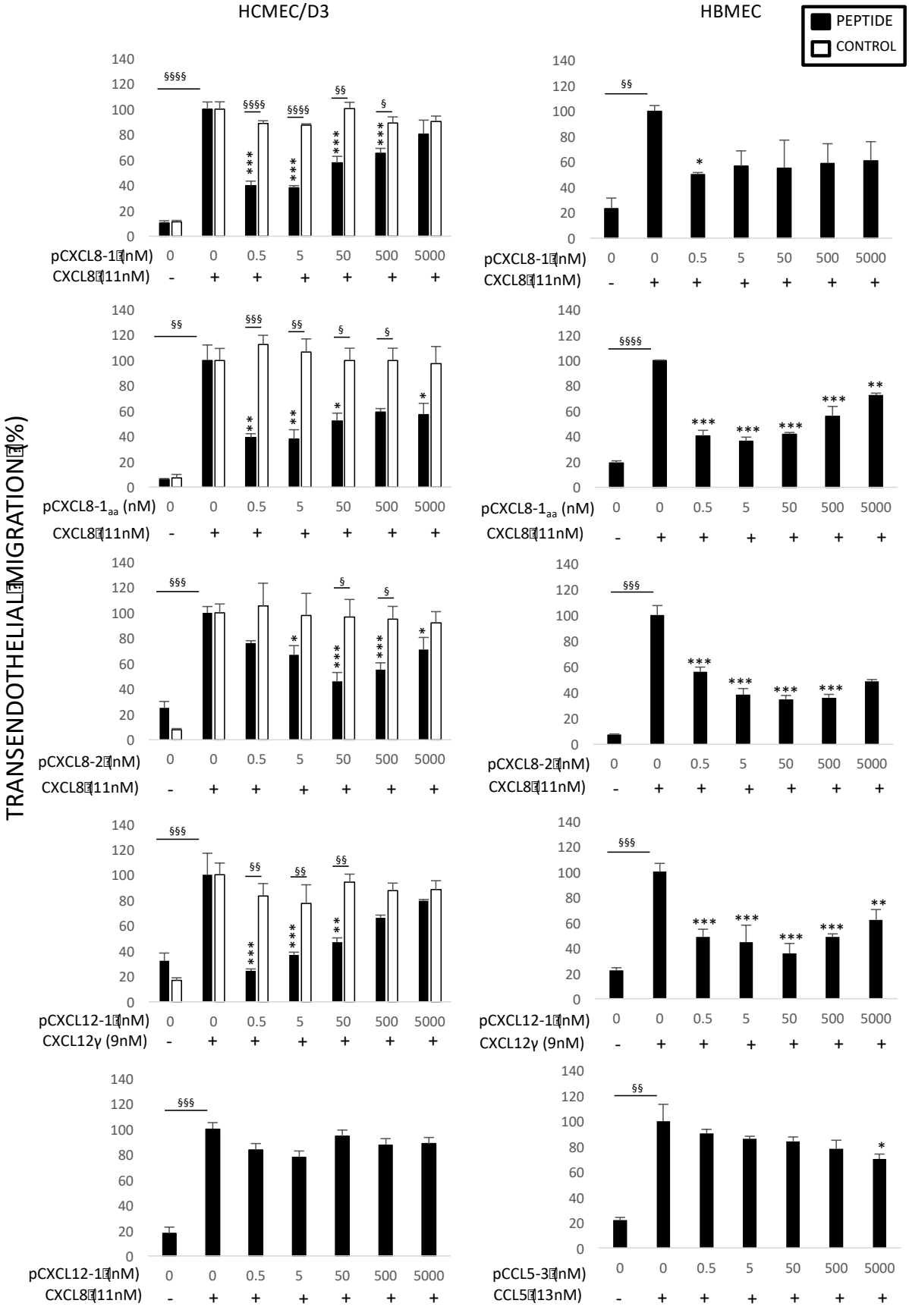
HCMEC/D3
HBMEC
PEPTIDE
CONTROL
TRANSENDOTHELIAL MIGRATION (%)
pCXCL8-1 (nM)
CXCL8 (11nM)
pCXCL8-1aa (nM)
pCXCL8-2 (nM)
pCXCL12-1 (nM)
CXCL12γ (9nM)
pCCL5-3 (nM)
CCL5 (13nM)
0 0 0.5 5 50 500 5000
- + + + + + +

Figure 5

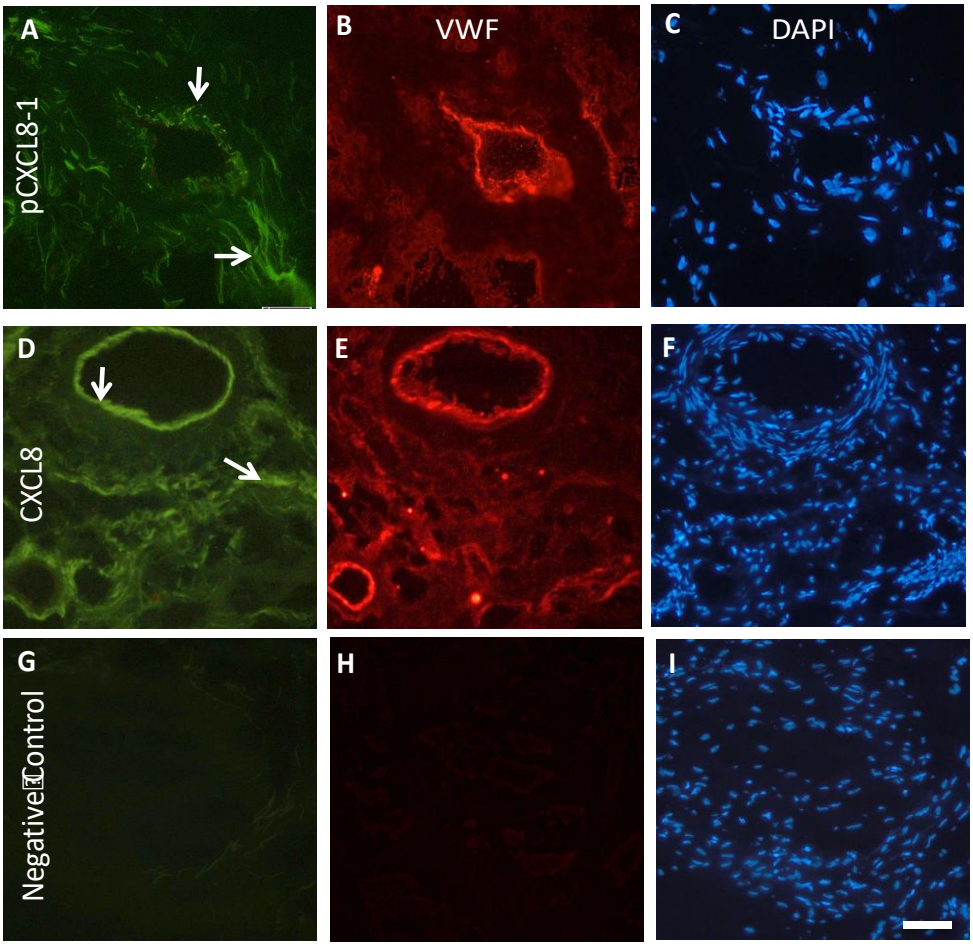

Figure 6

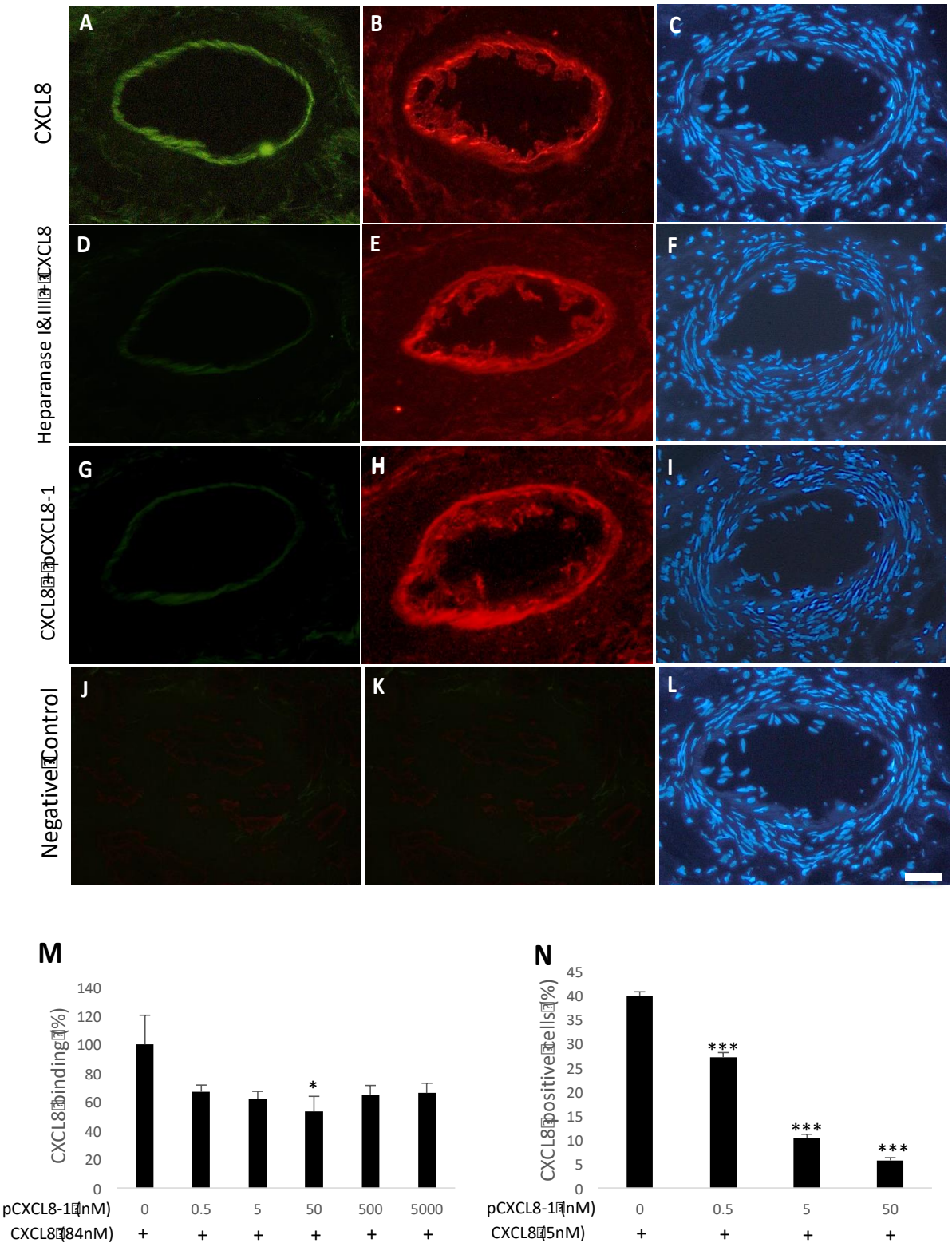
A
B
C
CXCL8
D
E
F
Heparanase I&III+CXCL8
G
H
I
CXCL8+pCXCL8-1
J
K
L
Negative Control
M
CXCL8 binding (%)
140
120
100
80
60
40
20
0
*
pCXCL8-1 (nM)
0
0.5
5
50
500
5000
CXCL8 (84nM)
+
+
+
+
+
+
N
CXCL8 positive cells (%)
45
40
35
30
25
20
15
10
5
0
***
***
***
pCXCL8-1 (nM)
0
0.5
5
50
CXCL8 (5nM)
+
+
+
+

Figure 7

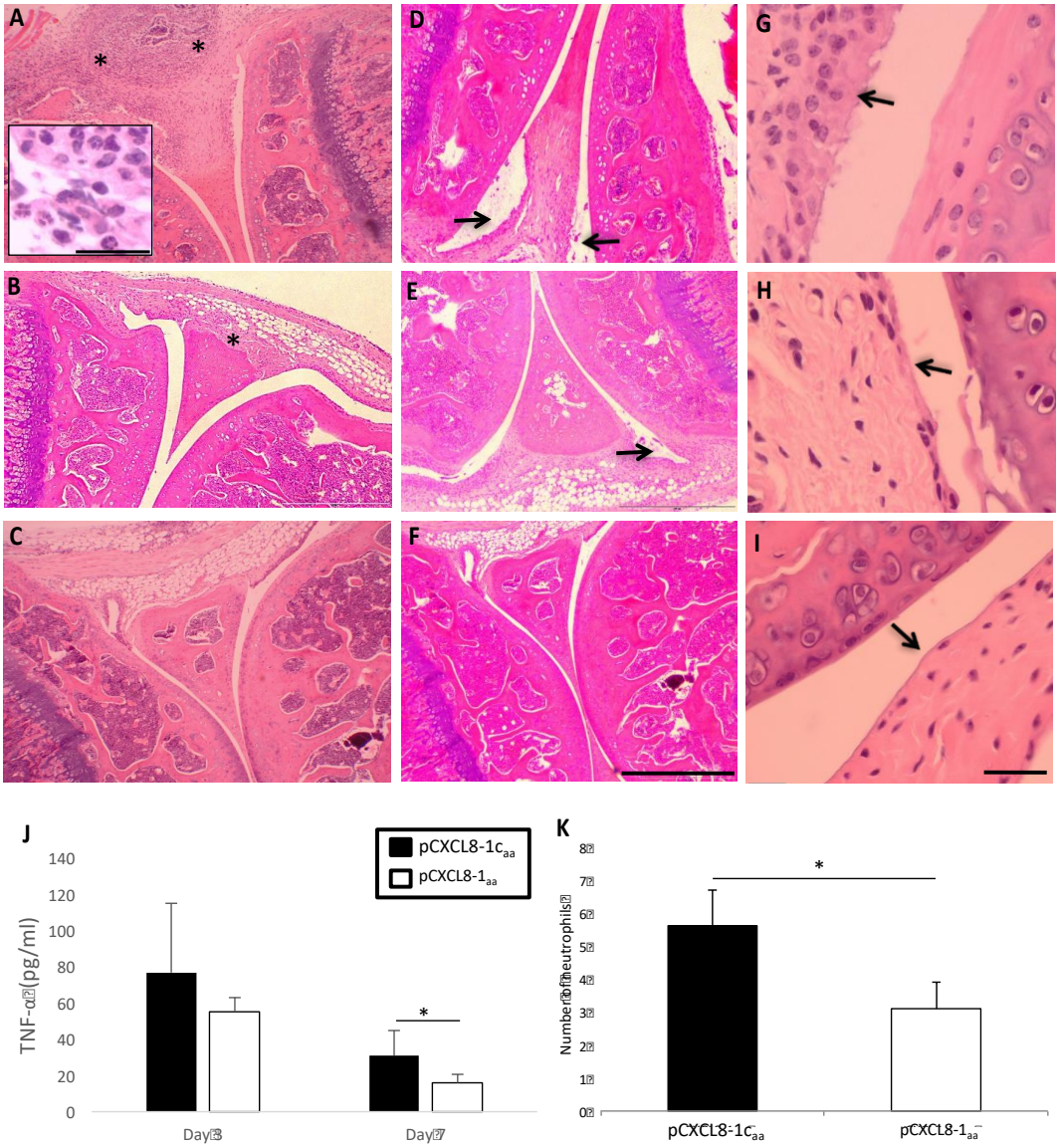
A
D
G
B
E
H
C
F
I
J
TNF-α (pg/ml)
140
120
100
80
60
40
20
0
pCXCL8-1c$_{aa}$
pCXCL8-1$_{aa}$
*
Day 3
Day 7
K
Number of neutrophils
8
7
6
5
4
3
2
1
0
*
pCXCL8-1c$_{aa}$
pCXCL8-1$_{aa}$

Supplementary Figure 1